



Review

Membrane Protein Modified Electrodes in Bioelectrocatalysis

Huijie Zhang [†], Rosa Catania [†]  and Lars J. C. Jeuken ^{*†} 

School of Biomedical Sciences and the Astbury Centre for Structural Molecular Biology, University of Leeds, Leeds LS2 9JT, UK; H.Zhang6@leeds.ac.uk (H.Z.); R.Catania@leeds.ac.uk (R.C.)

* Correspondence: L.J.C.Jeuken@leeds.ac.uk; Tel.: +44-113-343-3829

[†] These authors have contributed equally.

Received: 18 November 2020; Accepted: 3 December 2020; Published: 6 December 2020



Abstract: Transmembrane proteins involved in metabolic redox reactions and photosynthesis catalyse a plethora of key energy-conversion processes and are thus of great interest for bioelectrocatalysis-based applications. The development of membrane protein modified electrodes has made it possible to efficiently exchange electrons between proteins and electrodes, allowing mechanistic studies and potentially applications in biofuels generation and energy conversion. Here, we summarise the most common electrode modification and their characterisation techniques for membrane proteins involved in biofuels conversion and semi-artificial photosynthesis. We discuss the challenges of applications of membrane protein modified electrodes for bioelectrocatalysis and comment on emerging methods and future directions, including recent advances in membrane protein reconstitution strategies and the development of microbial electrosynthesis and whole-cell semi-artificial photosynthesis.

Keywords: membrane protein; bioelectrocatalysis; electrode modification; biofuel cells; photosynthesis; liposomes; hybrid vesicles; microbial electrosynthesis

1. Introduction

Membrane proteins constitute 20–30% of all proteins encoded by both prokaryotic and eukaryotic cells. They perform a wide variety of functions, including material transport, signal transduction, catalysis, proton and electron transport (Figure 1) [1]. They are also key to a number of earth's most fundamental reactions, such as respiration and photosynthesis [2,3]. Redox enzymes in the respiratory chain catalyse a variety of fundamental processes for energy conversion and fuel production, including H₂ oxidation, O₂ reduction, and carbon and nitrogen cycling. Membrane proteins that are involved in the light reaction of photosynthesis harvest light and facilitate electron transfer essential for solar energy conversion. The amphiphilic nature of membrane proteins makes them difficult to isolate, study and manipulate. Despite these challenges, membrane proteins have been widely advocated and studied for applications in bioelectrocatalysis, such as biofuel cells [4] and semi-artificial photosynthesis [5]. Here, we will review electrochemical studies of membrane proteins with the view to using these systems for bioelectrocatalysis. To aid discussion later on, we will briefly introduce a small selection of membrane enzymes active in bioenergy conversion, although this is far from a comprehensive list. We will then summarise the main strategies to immobilise membrane proteins on electrodes and discuss common techniques used to characterise these electrodes, including electrochemistry, spectroscopy, spectroelectrochemistry, microscopy and quartz crystal microbalance. Finally, some critical application challenges and potential future research directions will be highlighted that might find application in bioelectrocatalysis. Specifically, we will focus on two emerging directions. One is the reconstitution of membrane proteins into hybrid vesicles to extend their functional lifetime. The other is the use of microorganisms for microbial electrosynthesis and semi-artificial photosynthesis.

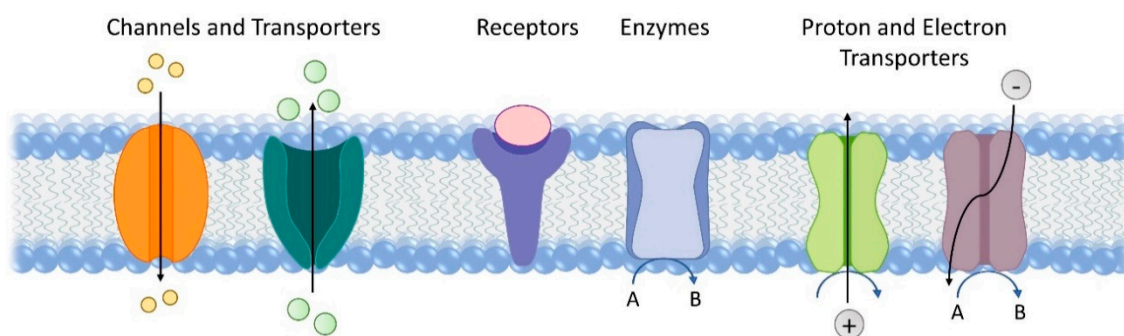


Figure 1. Representative functions of transmembrane proteins.

2. Membrane Proteins in Biofuel Conversion and Photosynthesis

2.1. Membrane Enzymes in Biofuel Conversion

Nature offers highly specialised enzyme machineries that can be exploited for (bio)fuel conversion. Among them, membrane-bound hydrogenases, found in many bacteria, archaea and lower eukaryotes, are metalloenzymes capable of catalysing the reversible oxidation of H_2 to protons and electrons [6]. Depending on the metal located in the active site, three phylogenetically unrelated classes can be identified: [NiFe], [FeFe] and, less common, [Fe] hydrogenases. Most hydrogenases are rapidly and almost completely inactivated by O_2 [7]. However, aerobic or facultative aerobic H_2 -oxidising bacteria have a particular subtype of O_2 -tolerant [NiFe] hydrogenase, which withstands the presence of O_2 and are membrane-bound hydrogenases (MBHs) [8]. The most studied O_2 -tolerant [NiFe] hydrogenases are found in *Ralstonia eutropha*, *Ralstonia metallidurans*, *Aquifex aeolicus*, *Hydrogenovibrio marinus* and *Escherichia coli*. MBHs are multimeric proteins with one large subunit and one small subunit, bound to the periplasmic side of the cytoplasmic membrane through a transmembrane protein (*b*-type cytochrome) [8]. The [NiFe] active site, with the same configuration as other [NiFe] hydrogenases, is deeply buried in the large subunit. MBHs couple oxidation of hydrogen in the large subunit to the reduction of either menaquinone-7 or ubiquinone-8 in the *b*-type cytochrome in the membrane.

In the respiratory chain, terminal oxidases catalyse the reduction of molecular oxygen to water without formation of reactive oxygen species (ROS). They oxidise quinones (ubiquinone and menaquinone oxidases) or cytochromes (cytochrome *c* oxidases) and can be classed into haem-copper oxidases [9], *bd* oxidases [10] or alternative oxidases [11]. For instance, cytochrome *bo*₃ enzymes are haem-copper oxidases in bacteria such as *E. coli* and couple oxidation of ubiquinol-8 to the reduction of oxygen [12]. Cytochrome *bd* is a quinol-dependent terminal oxidase found exclusively in prokaryotes and is structurally unrelated to haem-copper oxidases [13].

Nitrate reductases are molybdoenzymes capable of reducing nitrate (NO_3^-) to nitrite (NO_2^-). This enzyme family can be found in eukaryotic and prokaryotic cells. Eukaryotic nitrate reductases are present in plants, algae and fungi, and are involved in the assimilation of nitrate. Prokaryotic nitrate reductases are classified into three classes: assimilatory nitrate reductases (Nas), periplasmic nitrate reductases (Nap) and respiratory nitrate reductase (Nar). The latter are transmembrane enzymes which use nitrate as the electron acceptor of an anaerobic respiratory chain [14]. Facultative anaerobic bacteria use these alternative respiratory enzymes in oxygen depleted environments, replacing oxygen with different electron acceptors [15]. For instance, under anaerobic conditions, *E. coli* expresses a respiratory membrane-bound NarGHI coupled with a membrane-bound formate dehydrogenases (FDH-N). These two membrane enzymes form the supermolecular formate:nitrate oxidoreductase system. FDH-N oxidises formate to CO_2 , after which electrons are transferred to nitrate with the formation of a proton-motive force across the cytoplasmic membrane [16].

2.2. Membrane Proteins in Photosynthesis

Photosynthesis is the natural process by which photosynthetic organisms convert light energy into chemical forms. The key steps, which include light harvesting, charge separation and electron transport, occur in the membrane. For oxygenic photosynthesis in algae, higher plants and cyanobacteria, two photosynthetic complexes are involved: photosystem I (PSI) and photosystem II (PSII) [17], each with a peripheral antenna system: light harvesting complex I (LH I) for PSI and light harvesting complex II (LH II) for PSII [18]. Anoxygenic photosynthesis in bacteria, such as purple bacteria, is conducted by just one type of photosystem [19]. There are two types of light-harvesting complexes in most purple bacteria. The light-harvesting complex I and reaction centre forms the RC-LH I complex which is surrounded by multiple light-harvesting complex II [20]. In both oxygenic and anoxygenic photosynthesis, light-harvesting complexes exert the vital function to effectively absorb light and transfer the energy to the reaction centres [21]. Light-harvesting complexes absorb a limited spectral range depending on their natural pigment. The light-induced charge separation occurs at the reaction centres: PSII catalyses the light-driven water oxidation to reduce quinones, while the reaction centre of purple bacteria only catalyses the reduction of quinones (part of the cyclic electron transfer process). PSI is not catalytically active but instead serves as an “electron pump” which can be potentially coupled to the other redox catalysts. Electrodes interfaced with photosynthetic proteins have found broad applications in biosensors, biophotovoltaic cells and solar fuels generation [5,22,23].

3. Membrane Protein Electrode Design

Redox enzymes are molecular electrocatalysts that can function either in solution or while immobilised on an electrode surface. Immobilising enzymes on the electrodes has several advantages for electrocatalysis and this review will consider only immobilised systems. It is important that the enzymes retain their structural integrity and catalytic activity upon immobilisation [24]. Unlike soluble proteins, transmembrane proteins exist within lipid membranes and, consequently, are less stable in an aqueous environment where the amphiphilic properties of membrane proteins can lead to aggregation and denaturation. Therefore, it is challenging to retain the stability and function of membrane proteins in *in vitro* studies [25]. Suitable detergents or mixed lipid/detergent systems are needed to maintain an amphiphilic environment surrounding the membrane protein and mimic the original membrane conditions [26,27]. Alternatively, for some multisubunit, heteromeric membrane proteins the solubility problem can be circumvented by either purifying only the soluble subunits or engineering the protein to express only the soluble subunits [28]. For instance, the large and small subunits of membrane-bound hydrogenases can be separated from the transmembrane “anchor” subunit (*b*-type cytochrome). More sophisticated approaches have been developed for the mammalian membrane-bound cytochrome P450 that has been bioengineered without the hydrophobic membrane anchor domain [29]. However, similar methods are not always applicable for other proteins, either because the catalytic centre is located in a polytopic membrane subunit or because the water-soluble subunits on their own are not stable. It is worth mentioning that the activity of certain membrane proteins can be dependent on the presence of particular annular lipids [30] and therefore the strategies that improve the solubility by removing the need of the membrane environment can have some potential downsides.

Various immobilisation methods have been developed to achieve efficient electron transfer between a membrane protein and an electrode. There are several aspects to consider when designing and assembling (membrane) protein modified electrodes for bioelectrocatalysis: (1) orientation of the protein on the electrode surface, (2) preservation of the protein structural integrity and functionality, (3) low overpotential to minimise the energy loss, (4) protein loading of the electrode [24,31,32]. Some methods developed for electrocatalysis using soluble proteins can be adapted to detergent solubilised membrane proteins. An alternative strategy to the use of detergent is represented by reconstitution of membrane proteins within a lipid membrane on the electrode surface and several strategies have been developed to achieve this. We will discuss the most commonly used immobilisation methods.

3.1. Unmodified Electrode

Detergent solubilised membrane proteins can be absorbed directly on carbon, metal or semi-conductor electrodes in an approach known as protein film electrochemistry (Figure 2a) [33]. A frequently used electrode material is pyrolytic graphite “edge” (PGE) which has a rough, negatively charged surface, which can be tailored with polycations such as polymixin B or poly-L-lysine if required. Respiratory nitrate reductase (NarGHI) isolated from *Paracoccus pantotrophus* in *n*-dodecyl β -D-maltoside (DDM) buffer was adsorbed onto PGE electrodes and showed direct electron transfer (DET) with the electrode [34]. The catalytic activity of NarGHI from *E. coli* was studied over a wide pH range ($5 < \text{pH} < 9$), nitrate concentrations and in the presence of inhibitor [35]. Similarly, purple bacteria RC-LH I was solubilised in 0.1% lauryldimethylamine N-oxide (LDAO) buffer and immobilised directly on a bare Au electrode [36]. RC-LH I did not exhibit DET, but showed photocurrents ($\sim 64 \text{ nA/cm}^2$) when ubiquinone-0 and cytochrome *c* were present in solution, indicating that electron transfer needs to be mediated by small redox compounds in this system (mediated electron transfer, MET). Like water-soluble proteins, membrane proteins on bare electrodes often lack a specific orientation and this can impede efficient electron transfer between electrode and proteins. Making use of the amphiphilic nature of membrane proteins, a densely packed protein monolayer with defined orientation can be formed on electrode surfaces by Langmuir–Blodgett deposition and this was shown to increase the electron transfer efficiency [37–41]. An example of this strategy can be found in Kamran et al. where detergent solubilised-RC-LH I was first pre-assembled in a monolayer at a water-air interface and then transferred onto a gold-coated electrode, reaching photocurrent values of $\sim 45 \mu\text{A/cm}^2$ [37].

3.2. SAM Modified Electrode

An electrode surface can be modified to promote protein immobilisation and control the orientation of the protein on the surface. A common method to functionalise metallic electrode surfaces, in particular gold electrodes, is to form a self-assembly monolayer (SAM) of thiols (e.g., alkanethiols) (Figure 2b). By changing the length of the thiol compound (e.g., the alkyl chain), the distance between the protein and electrode can be controlled. More importantly, by changing the terminal group of the SAM (e.g., *n*-hydroxy-alkanethiol or *n*-amino-alkanethiol), the surface chemistry of the electrode can be controlled. As protein binding to surfaces is typically governed by van-der-Waals and electrostatic interactions, the surface chemistry strongly influences the orientation of proteins on the surface [42,43].

Besides tuning the chemistry of the electrode surface, proteins can be genetically engineered to control their orientation on the electrode through affinity interactions. RCs from *Rhodobacter sphaeroides* in LDAO detergent have been immobilised on SAM-modified electrodes terminated by Ni-NTA groups. By genetically engineering a poly-histidine tag (His7) at the C-terminus of the M-subunit of the RC, the primary donor of RC was positioned to face the electrode [44]. The histidine tag can also be engineered on H subunit of RCs to achieve the opposite orientation [45]. The Ni-NTA modified gold electrodes have also been used to immobilise His-tagged PSII solubilised in DDM buffer [46]. A different strategy that has been explored is to modify the gold electrode surface with an amine terminated SAM for further reaction with terephthalaldehyde (TPDA). The TPDA modified SAM reacts with lysine residues from PSI to form covalent imine bonds [47]. Such an approach does not create the same orientational control compared to the His-tag/NTA coupling. Irrespective of selective orientation on the surface, mediators are often required for efficient electron exchange with membrane proteins. Small proteins like cytochrome *c* are widely used as mediators for PSI and purple bacteria RC [48]. Water-soluble redox mediators such as 2,6-dichloro-1,4-benzoquinone (PSII), 2,6-dichlorophenolindophenol (PSI), sodium ascorbate (PSI) and ferricyanide (PSI) are also commonly used to facilitate efficient electron transfer between the protein and electrode [49].

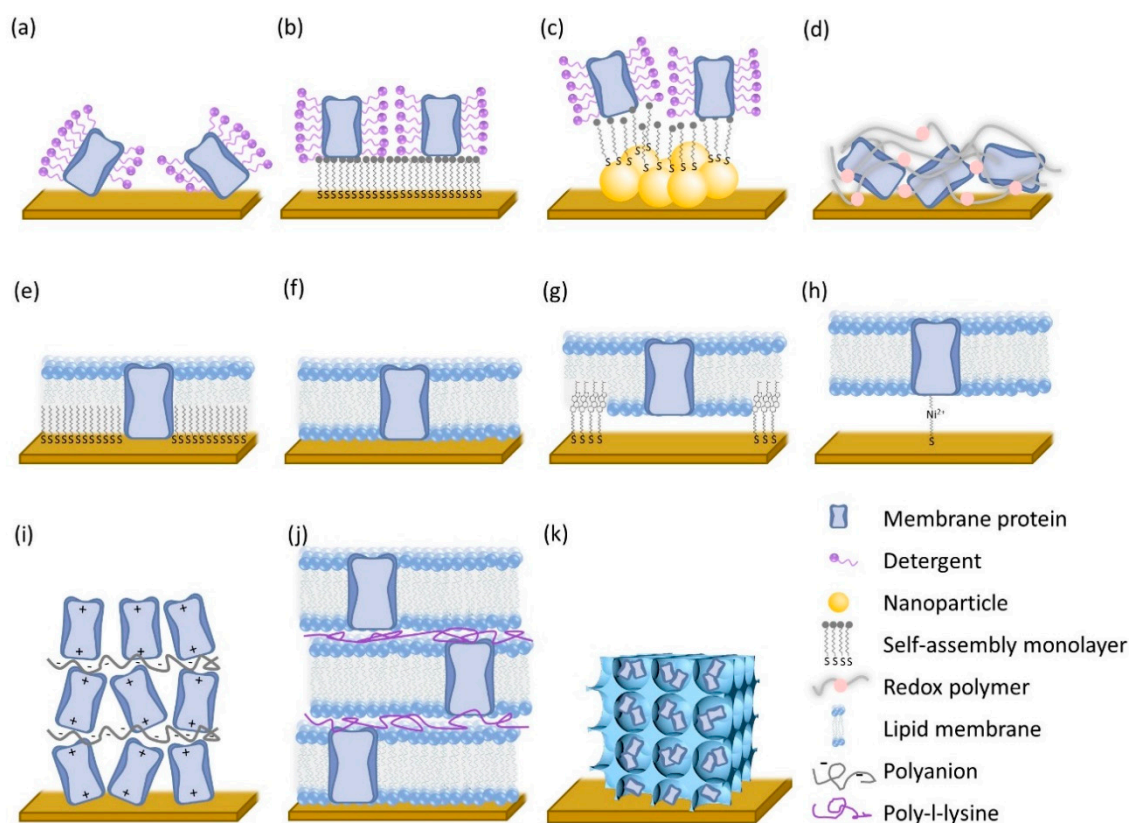


Figure 2. Overview of the strategies for membrane protein modified electrodes (not to scale). Proteins absorbed on (a) an unmodified electrode, (b) a SAM modified electrode and (c) a nanoparticle modified electrode. (d) Immobilisation of membrane proteins within a redox polymer. Examples of lipid membrane-modified electrodes: (e) a hybrid bilayer lipid membrane (hBLM), (f) a solid supported bilayer lipid membrane (sBLM), (g) a tethered bilayer lipid membrane (tBLM) and (h) a protein tethered bilayer lipid membrane. (ptBLM). (i) Layer-by-layer deposition of alternating charged films. (j) Multilayered lipid membrane stacks. (k) 3D structure electrode for protein immobilisation.

3.3. Nanoparticle Modified Electrode

Nanoparticles (NPs) have been shown to enhance interfacial electron transfer between a variety of electrodes and proteins [50] and gold NP-modified electrodes have been successfully used to study membrane proteins (Figure 2c), such as terminal oxidases: *E. coli* cytochrome *bd* (a quinol oxidase) [51], *Paracoccus denitrificans* cytochrome *aa₃* [52] and *Thermus thermophilus* cytochrome *ba₃* [53] (two cytochrome *c* oxidases). The use of NPs facilitated DET between the electrode and protein, enabling more in-depth studies on enzyme activity. The size of the NPs significantly affects the electron transfer rates and smaller particles reduced the requirement of overpotential for O₂ reduction activity by *E. coli* cytochrome *bo₃* [54]. The group of Hellwig has recently studied the role of the surface charge of thiol-modified gold NPs, the length of the thiols and the effect of phospholipid composition on the interaction and DET between NP and the membrane enzyme, cytochrome *bd* [55]. Both cytochromes *bo₃* and *bd* used in the aforementioned studies were isolated and stabilised in DDM buffer. Besides gold NP, various other particles have been used for protein immobilisation [56]. The Armstrong group used graphite microparticles to pair electron donor and acceptor membrane enzymes [57]. [NiFe] membrane-bound hydrogenase was reconstituted with either *E. coli* nitrate reductase (NarGHI) or *E. coli* fumarate reductase (FrdAB; not a membrane protein) on single microparticles; both systems catalysed the reductions of nitrate or fumarate, respectively, by hydrogen. In 2015, Duca et al. [58] demonstrated a cascade electrochemical reduction of nitrate to ammonia by immobilising *E. coli* respiratory nitrate reductase (NarGHI) on an electrode (in polyoxyethylene 9-dodecyl ether detergent) with Pt or Rh nanoparticles.

3.4. Redox Polymers

Redox polymers are widely used for wiring redox proteins on electrode surface (Figure 2d) [59]. Redox polymers act simultaneously as immobilisation matrix and as redox mediators. High coverages of proteins can be achieved and the ubiquitous localisation of redox mediators bound to the polymer matrix negates the need to control protein orientation. These polymer-bound redox mediators overcome mass transport limitations, typically observed with freely diffusing redox mediators. The chemical and physical properties of the redox polymers can be tailored by tuning the polymer backbone and the redox mediators. The Schuhmann group has extensively explored Os redox polymers to “wire” DDM-solubilised PSI [60] and PSII [61] on electrode surfaces for photocurrent generation. A two-compartment cell with a PSII photoanode and a PSI photocathode was constructed to mimic the Z-scheme of natural photosynthesis and an open-circuit voltage (OCV) of 90 mV was achieved [62]. By tuning the redox potential of Os complexes in the redox polymers to match the redox sites of the proteins (PSII and PSI), the OCV could be increased from 90 mV to 372 mV [63]. Interestingly, by exploiting the pH-dependent properties of Os-modified polymer, the group of Plumeré improved the interfacial electron transfer rates for the PSI photocathode, even exceeding rates observed in natural photosynthesis [64].

3.5. Membrane Modified Electrode

Because of the nature and functions of the membrane proteins, it is important that their assembly on electrodes preserves their structural integrity and functionality. In the examples provided so far, detergents are used to retain stability of the immobilised membrane enzymes. Although detergents are required to accommodate the amphiphilic nature of membrane proteins, they also have adverse effects to membrane protein stability and are likely to influence the electrode-protein interaction. To mimic the native environment of membrane proteins, electrodes have been modified with model membranes, as reviewed previously [65–67]. These membrane-modified electrodes can be categorised into hybrid bilayer lipid membrane (hBLM) system (Figure 2e), solid supported bilayer lipid membrane (sBLM) system (Figure 2f), tethered bilayer lipid membrane (tBLM) system (Figure 2g), and protein tethered bilayer lipid membrane (ptBLM) system (Figure 2h).

In hBLM systems a phospholipid layer is absorbed onto a self-assembled monolayer (SAM) of alkylthiols (Figure 2e). This strategy was used by the Hawkrigge group to study cytochrome *c* oxidase immobilised on gold electrode [68,69]. In sBLMs, a lipid bilayer is non-covalently bound to the electrode surface (Figure 2f). Photosynthetic reaction centres including *Rhodobacter sphaeroides* RC [70,71], spinach photosystem I [72] and photosystem II [73] have been integrated into sBLMs on pyrolytic graphite. Electron transfer between electrode and the aforementioned proteins was achieved and showed well-defined peaks in voltammetry which corresponded to the redox sites of the proteins. Noji et al. incorporated *Rhodospseudomonas palustris* RC-LH I into sBLMs on an ITO electrode. Anionic phospholipid like phosphatidylglycerol (PG) were shown to stabilise the charge-separated state of RC-LH I and enhance the photocurrent [74]. In tBLM systems, the membrane is ‘tethered’ to the lipid-modified electrode surface via a linker (Figure 2g). Cytochrome *bo*₃ has been incorporated into tBLMs and was shown to retain its catalytic activity [75]. We previously included the membrane-bound [NiFe]-hydrogenases (MBH) from *R. eutropha* into a tBLM approach and used electrochemistry to study the activity of the entire heterotrimeric membrane-bound form of the enzyme [76]. In 2016, Pelster and Minter isolated mitochondrial electron transport chain (ECT) enzymes, reconstituted them into liposomes and immobilised them onto a gold electrode in a tBLM. The authors used this reconstructed mitochondrial inner membrane biomimic to show the interdependence of the different complexes on bioelectrocatalytic activity [77]. In ptBLMs, the membrane protein is first anchored to an electrode via a His-tag/NTA interaction and subsequently reconstituted into a lipid membrane (Figure 2h). Ataka et al. have immobilised the *Rhodobacter sphaeroides* cytochrome *aa*₃ (a cytochrome *c* oxidase) by using a ptBLM system [78–80]. Two opposite protein orientations were compared, by varying the position of the His-tag. Cytochrome *c* bound and exchanged electrons with cytochrome *c* oxidase only when

the latter was orientated with its subunit II (the binding domain for cytochrome *c*) facing the bulk aqueous medium.

3.6. Multi-Layer Assembly, Multilayered Lipid Membrane Stacks, 3D Structure Electrode

An important aspect to improve the performance of bioelectrocatalysis is catalyst loading on the electrode surface. For membrane proteins, this can be achieved via two alternative strategies: multi-layer (membrane) assembly (Figure 2d,i,j) and/or 3D electrode structure (Figure 2k). For a more detailed discussion on layer-by-layer assembly approach for redox proteins, we also refer to [65,81]. Multilayer immobilisation within a redox polymer matrix was already discussed in Section 3.4. As an example of a layer-by-layer approach (Figure 2i), PSI has been co-assembled with cytochrome *c* as mediator using DNA as an anionic polymer [82]. The purple bacteria RC was also co-assembled into a multilayer architecture by alternating layers of RC with a cationic polymer poly(dimethyldiallylammonium chloride) (PDDA) [83,84]. Our group used poly-L-lysine (PLL) as an electrostatic polymer to construct multilayered lipid membrane stacks (Figure 2j) [85,86]. Two membrane proteins, *E. coli* cytochrome *bo*₃ and *R. eutropha* MBH, were incorporated into these lipid membranes stacks. Lipophilic quinones, the natural substrates of cytochrome *bo*₃ and MBH, diffuse freely between the multilayered membranes and mediated electron transfer between the proteins and the electrode. Catalytic activity was shown to increase linearly with the number of membrane layers for at least up to 5 layers [86].

The high surface area of so-called 3D electrodes can be used to immobilise proteins at high loading [87]. Mesoporous metal electrodes have been shown to increase protein loading compared to planar electrodes, e.g., rough silver electrode for bacteria RC [88] and nanoporous gold electrode for PSI [89]. A mesoporous WO₃-TiO₂ film electrode has been reported for the entrapment for bacterial RCs [90] and mesoporous indium tin oxide (ITO) electrodes have been used to immobilise PSII [91]. The ITO electrode can be modified with SAM to covalently bind and orientate PSII with the electron acceptor side of towards the electrode surface, enhancing electron transfer kinetics and electrode stability [92]. A hierarchically structured, inverse opal, mesoporous (IO-meso) ITO electrode was later developed to provide even larger surface areas [93]. These electrodes were combined with redox polymers to electrically wire PSII with the 3D structure of IO-meso ITO, yielding photocurrent densities of up to ~410 $\mu\text{A cm}^{-2}$ [94]. Mesoporous ITO electrodes were also applied to co-immobilise cytochrome *c* and PSI and photocurrent densities >150 $\mu\text{A}\cdot\text{cm}^{-2}$ were achieved [95]. The effect of pore size was studied by comparing photocurrents between mesoporous (20–100 nm) and macroporous (5 μm) electrodes using 2,6-dichlorophenolindophenol (DCPIP) and ascorbate as redox mediator for PSI. The macroporous electrode showed three times higher photocurrent than the mesoporous electrode [96]. The authors observed that the macroporous electrode increased the active surface area twice compared to the mesoporous electrode with the same PSI mass loading. They concluded that the increase in photocurrent was due to multilayers of PSI deposited along pore walls and the macropores enhanced the MET within a single pore.

4. Methods to Characterise Membrane Protein Modified Electrode

The characterisation of electrodes and protein films is very often achieved through a combination of powerful and advanced techniques and their combination with electrochemical tools. In this section, we will focus on the most commonly used techniques to study membrane proteins on electrode surfaces and we will report some representative works.

4.1. Electrochemical Methods

Protein film electrochemistry (PFE) is a well-established and important technique to study protein modified electrodes and has proven powerful to probe the thermodynamic, kinetic and catalytic properties of redox proteins, typically with voltammetry [97–99]. PFE is also compatible with membrane-modified electrode and allows to probe the membrane proteins within detergent solutions,

polymer matrices or model-membrane environment [100,101]. We refer to the following reviews for a detailed description of PFE methods [102–106].

Besides voltammetry, impedance spectroscopy has been used to study the electrode-membrane protein interface. The quality and the structure of electrode surfaces modified with planar lipid membranes (Figure 2e–h) are particularly suitable for investigation by electrochemical impedance spectroscopy (EIS). EIS can monitor the resistance and the capacitance of a planar membrane covering the electrode. For ideal planar lipid bilayers on the electrode, the capacitance value should be in the range of $\sim 0.5 \mu\text{F}\cdot\text{cm}^{-2}$ with a resistance of $> \text{M}\Omega \text{ cm}^2$ [107]. Disorders and defects of these bilayers will result in lower resistance and/or higher capacitance values. For instance, we monitored the formation of multilayer membrane stacks (Figure 2j) by EIS [86] and observed only small reductions in capacitance upon the formation of each additional bilayer, indicating that the additional lipid bilayers permeable to ions and thus contain large or many defects. EIS can also provide information on whether protein incorporation in the membranes affects the electrode structure. For instance, incorporation of cytochrome b_0_3 into tethered membranes (tBLM, Figure 2g) had almost no effect on the capacitance, indicating that cytochrome b_0_3 did not induce large defects in the tBLM [75]. Similarly, only small changes in capacitance were observed of a hBLM (Figure 2e) after integrating human enzyme cytochrome P450, indicating that the hBLM retains its integrity upon protein adsorption [108]. Besides the membrane, the quality of a SAM on metal electrodes is also often evaluated with EIS. Compact, well-formed SAMs act as ideal insulating layers with high resistance values. The compactness of the SAM will influence subsequent protein immobilisation steps and can determine the thickness of the SAM, impacting on interfacial electron transfer kinetics.

Protein-film photoelectrochemistry (PF-PEC) is a PFE technique which has been developed for photosynthetic proteins [22,109–111]. PF-PEC combines illumination with PFE to investigate photoactive proteins. Voltammetry and chronoamperometry can be used to illustrate the charge transfer processes and the kinetics of the light driven reactions. Recently, other electrochemical setups have been used to investigate photosynthetic proteins, including rotating ring disk electrode (RRDE) and scanning electrochemical microscopy (SECM). The set-up of RRDE includes a central rotating disc electrode and a ring electrode surrounding it. The potential on these two electrodes can be controlled independently and products generated by a protein film at the central disk electrode are transferred to the ring electrode for electrochemical analysis. For instance, oxygenic photoreactivity of PSII was studied with RRDE [112] and products generated by PSII at the central disc, e.g., oxygen and radical species, were detected by the ring electrode. This study revealed ET pathways that generate reactive oxygen species and O_2 by PSII. SECM employs a microelectrode as a tip above the protein modified electrode to detect the products generated locally. It was used to monitor H_2 evolution of a PSI-Pt complex within redox polymer under illumination [113]. SECM has also been used to quantify the reduction of charge carriers (methyl viologen) by PSI and compared this to the photocurrent [114]. Methyl viologen is often used as a charge carrier to collect electron from PSI in biophotovoltaic systems, but reoxidation on the electrode leads to charge recombination. The authors compared PSI on gold and silicon surfaces, both with Os-based redox polymers. SECM showed that gold and silicon exhibits different photocurrents due to different charge recombination kinetics, i.e., electron transfer kinetics for the reoxidation of the methyl viologen radical cation. Finally, by monitoring the photocurrent and H_2O_2 generation of a PSI photocathode with SECM, it was shown that light-induced formation of reactive oxygen species caused degradation of PSI modified electrodes [115].

4.2. Spectroscopic Methods

While electrochemical methods provide information about redox reactions, in situ spectroscopic methods can be applied to characterise the structure of the protein and the electrode assembly. Surface-enhanced Raman spectroscopy (SERS) is a surface-sensitive technique for molecules and proteins immobilised on roughened metallic surfaces, in particular Ag [116]. The SERS effect is due to a large increase in the Raman cross-section of molecules in contact with the metal surface, which is

enhanced at metallic nanostructured surfaces due to local surface plasmon resonance (LSPR) effects. SERS has been used to successfully characterise oxidised and reduced forms of adsorbed cytochromes (cytochrome *c*, haemoglobin and myoglobin) under precise potential control with low laser power [117]. In 2005, Hrabakova et al. showed that no structural changes occurred to the haem sites (e.g., *a* and *a*₃) of cytochrome *c* oxidase embedded in a phospholipid bilayer tethered to a functionalised silver electrode via a histidine-tag [118]. In 2011, Weidinger group used SERS to study the electron transfer of MBH from *R. eutropha* H16 [119]. Interestingly, the authors compared the behaviour of the entire enzyme with just the transmembrane “anchor” subunit (*b*-type cytochrome) and determined two independent pathways for the electrons from the active site of the enzyme to the electrode. A slow rate pathway crosses all the three subunits of the enzyme, whilst a faster pathway only crosses two subunits and leaves out the transmembrane anchor subunit which, however, contributes to the stabilisation of the enzyme on the electrode.

A different variation of conventional infrared spectroscopy is represented by surface-enhanced infrared absorption spectroscopy (SEIRAS) in which the signal enhancement is due to plasmon resonance from a nanostructured metal thin film [120]. The Hellwig group used SEIRAS to characterise the deposition of gold NPs on gold electrodes, the modification of gold NPs with thiols and, finally, the absorption of cytochrome *bo*₃ on these modified electrodes [51,54]. Wiebalck et al. characterised the formation of a tBLM and incorporation of functional cytochrome *bo*₃ from *E. coli* by SEIRA spectroscopy [121].

4.3. Spectroelectrochemistry

Spectroelectrochemistry combines electrochemistry and spectroscopic approaches to monitor a specific molecular response while varying the electrode potential [122,123]. This can be done with proteins in solution [124] or immobilised on the electrode surface [125,126]. Insights into reaction mechanisms of membrane enzymes could be gained by methods such as UV-vis spectroelectrochemistry and infrared spectroelectrochemistry. UV-vis spectra of a protein are often specific for the redox state of a cofactor, e.g., haems, FeS clusters or flavins. A common application is a spectroelectrochemical titration to determine the reduction potential of a cofactor in an enzyme in solution, where results are usually evaluated by fitting the titration data to the Nernst equation. An example is a study of the cytochrome *bc*₁ complex where the midpoint potentials of the cofactors were determined by UV-vis and IR spectroelectrochemical titrations [127,128]. The redox potentials of the primary electron acceptor pheophytin *a* in photosystem II [129] and the primary electron donor P700 in photosystem I [130] were also revealed by UV-vis spectroelectrochemistry with proteins in solution. UV-vis spectroelectrochemistry can also be used to study proteins on electrode surfaces. For instance, Haas et al. used UV-vis spectroelectrochemical titrations to determine the midpoint potentials for cytochrome *c* oxidase either in solution or in a Langmuir-Blodgett monolayer film [131]. A multi-protein system was studied with UV-vis spectroelectrochemistry in which an outer-membrane cytochrome, MtrC from *Shewanella oneidensis* MR-1 (a peripheral membrane protein), was used as an electron conduit between an electrode and other redox enzymes. MtrC was shown to be an effectively transfer-electron conduit by monitoring the absorbance of reduced Fe^{II}-haems in MtrC [132].

Infrared (IR) spectroscopy is a powerful technique to detect structural changes of proteins during or in response to an electrochemical reaction although few studies have been reported for membrane proteins. Reactions can be triggered either by light or redox potential and infrared difference spectroscopy of proteins is typically measured to investigate the reaction mechanisms. This approach has been developed for membrane proteins involved in photosynthesis, respiration and metabolic pathways [100]. Electrochemical SEIRA was used to study the conformational changes of the *R. sphaeroides* cytochrome *c* oxidase induced by direct electron transfer in ptBLM system [133]. The cytochrome *c* oxidase was shown to change from a non-activated to an activated state after it involving enzymatic reaction. By applying periodic potential pulses switching between −800 mV and open circuit potential to control the state of cytochrome *c* oxidase, the kinetics of the conformational

changes was monitored by time-resolved SEIRA spectroelectrochemistry [134]. The bacterial respiratory ubiquinol/cytochrome b_0_3 couple was incorporated into a tethered bilayer lipid membrane (tBLM) on SAM modified electrode. The transmembrane proton gradient was successfully monitored by spectroelectrochemical SEIRA [121].

4.4. Microscopy

4.4.1. Electron Microscopy

Electron microscopy (EM) techniques are available to investigate membrane proteins (typically by cryo transmission electron microscopy, TEM or cryo-EM) and electrode structures (typically by scanning electron microscopy, SEM) at various scales. However, EM has not been widely used to study membrane proteins immobilised on electrodes as TEM and SEM are based on different modes of observation [135]. In 2015, Monsalve et al. [136] used SEM and TEM to characterise the morphology and size distribution of gold nanoparticles on a gold electrode used for direct absorption of *Aquifex aeolicus* [NiFe] membrane-bound hydrogenase surrounded by DDM detergent.

4.4.2. Atomic Force Microscopy

Atomic force microscopy (AFM) is a scanning probe microscopic technique based on a nanoprobe, a tip placed at the end of a long and narrow cantilever, that interacts with the sample surface to measure the topography of a surface [137]. Although AFM has been widely used to study lipid membranes [138–140], membrane proteins [141–144] and electrochemical systems with soluble proteins [145–147], AFM is less often used to study membrane proteins on electrode surfaces. In 2006, we used tapping-mode AFM to analyse the distribution of cytochrome b_0_3 on a tethered bilayer lipid membrane (tBLM) on stripped gold electrode [75]. AFM combined with Polarisation Modulation Infrared Reflection-Absorption Spectroscopy (PM-IRRAS) was used to study the different orientation of membrane-bound *Aquifex aeolicus* (Aa) [NiFe] hydrogenase immobilised on hydrophilic and hydrophobic SAM on gold electrodes. This work highlighted that on charged or hydrophilic interfaces, H_2 oxidation proceeds through both direct and mediated electron transfer processes, while on hydrophobic surfaces, a mediator is required [148]. In 2014, Gutiérrez-Sanz et al. [149] characterised the functional reconstitution of respiratory complex I on SAM on gold electrode. Their AFM study showed the formation of a phospholipid bilayer on SAM modified gold electrode and protrusions of 6–8 nm height were observed which were ascribed to the hydrophilic arm of complex I as this arm extends outside the membrane.

4.5. Quartz Crystal Microbalance

Quartz crystal microbalance (QCM) is a sensitive mass sensor which utilises acoustic waves generated by oscillating a piezoelectric, single crystal quartz plate to measure mass changes in the order of nanograms. The association of QCM with dissipation monitoring (QCM-D) allows to also measure the energy loss or dissipation (ΔD) of the system [150]. QCM was used to monitor the different stages of the ptBLM formation with cytochrome c oxidase from *Rhodobacter sphaeroides* as model protein [151]. The adsorption of cytochrome c oxidase at the surface decreased the resonance frequency while increased the dissipation. The Hawkrige group investigated the electrostatic association between cytochrome c and cytochrome c oxidase immobilised in hBLM with QCM [68,69]. The QCM data revealed the binding of cytochrome c and cytochrome c oxidase at different ionic strength which was related to the mediated electron transfer. QCM-D was also used to characterise the formation of the cystamine–pyrroloquinoline quinone–thylakoids layers onto SAMs [152].

5. Membrane Protein Modified Electrodes for Bioelectrocatalysis

The increased demand to produce energy and value-added chemicals from cheap and environmentally friendly renewable resources has driven the recent advances in bioelectrocatalysis research towards the development of alternative systems. The applications of bioelectrocatalysis range

from biosensors, energy conversion devices and bioelectrosynthesis [153–156]. The majority of the studies employ soluble proteins; however, some membrane proteins with suitable catalytic or electron transfer properties also find applications in bioelectrocatalysis. Some of them show advantages over soluble proteins or have unique functions. Here, we will discuss the membrane protein electrode applications in the field of bioelectrocatalysis.

5.1. Enzymatic Biofuel Cells (EBCs)

One of the most studied energy conversion devices is the enzymatic biofuel cell (EBC) which uses oxidoreductase enzymes as biocatalysts to convert chemical energy into electrical energy [157–159]. A typical EBC consists of a two-electrode cell in which the biofuels (such as H₂, formate) are oxidised at the bioanode and the oxidants are reduced at the biocathode (usually O₂ is reduced to water) [160]. Among these, H₂/O₂ biofuel cells are one of the most investigated enzymatic systems [161]. Hydrogenases are promising biocatalysts to fabricate high performance H₂-oxidation bioanodes. However, the extreme oxygen sensitivity of highly active hydrogenases is one of the main limitations of hydrogenase based H₂ bioanodes [162]. The O₂ sensitive hydrogenase can be protected by a low-potential viologen redox polymer matrix [163] or enzymatic O₂ scavenger [164]. However, these protection mechanisms either consume the electron from H₂ oxidation or add chemicals for protection. O₂-tolerant MBH therefore shows great advantage for H₂/O₂ biofuel cell. The first membrane-less H₂/O₂ cell was assembled by Armstrong group. Two pyrolytic graphite electrodes, coated respectively with MBH from *R. eutropha* and laccase from *Trametes versicolor* (*Tv*), were immersed in a H₂/air flushed solution. The system reached an OCV of ~970 mV and a maximum power output of ~5 μW [165]. High OCVs were achieved because MBH directly exchanged electrons with the electrode and no mediators were required. The *Re* MBH was solubilised from the membrane extracts by 2% Triton-X 114 and isolated via a *Strep*-tag sequence on the small subunit. It is possible that the MBH was devoid of the transmembrane cytochrome *b* anchor and this could explain why there was no need to use mediators. The *Re* MBH also showed CO-tolerance [165]. The same group further improved the performance of the H₂/O₂ cell by replacing the *Re* MBH with MBH (similarly *Strep*-tagged on the small subunit) from *R. metallidurans*, which is more active and stable to O₂ exposure (Figure 3a). The authors emphasised that such a system would have the advantage to perform H₂ conversion even in H₂-poor mixtures. They also showed that three cells in series provided a total OCV of 2.7 V which was sufficient to power a wristwatch for 24 h [166].

As described earlier, we have presented a strategy for using the full heterotrimeric MBH as a biocatalyst (including the cytochrome *b* anchor) and have used multi-layer membrane stacks on gold electrode to increase MBH loading [86]. In our approach, we used cytoplasmic membrane extracts of *R. eutropha* and created interconnected layers of membranes with each layer containing anchored MBHs. Lipophilic quinones were used as mediator, shuttling electron between electrode and protein. However, the irreversible electrochemical behaviour of the quinone redox reaction increases the required overpotential for H₂ oxidation, which will limit the power output of the devices and more research is needed to resolve this.

To optimise EBCs, gas diffusion electrodes have been investigated and enzyme coverage optimised. The porous structure of the gas diffusion electrode can increase the mass loading of the biocatalyst and overcome the mass transport limitation of gases. In 2016, Kano group used an O₂-tolerant MBH from *Hydrogenovibrio marinus* and an O₂-sensitive [NiFe]-hydrogenase from *Desulfovibrio vulgaris* “Miyazaki F” to create DET-type gas diffusion electrodes [167]. The authors did not specifically comment on whether their enzyme purification methods might have affected the presence of the cytochrome *b* anchor subunits of MBH. The MBHs were isolated through two different procedures. The large and small subunits of the O₂-tolerant MBH were isolated through detergent solubilisation and maintained in 0.025% Triton-X. The O₂-sensitive MBH went through a trypsinisation process which could lead to the separation of the transmembrane cytochrome *b* anchor. These H₂ oxidation electrodes generated a current density of 10 mA·cm⁻² in the half-cell configuration. Contrary to the O₂-tolerant MBH, the O₂-sensitive MBH did not show overpotential for H₂ oxidation and, on this basis, was selected

by the authors as bioanode of a H_2/O_2 EBC for a further study. Coupling this O_2 sensitive MBH anode with bilirubin oxidase (BOD) from *Myrothecium verrucaria* immobilised on Ketjen black-modified waterproof carbon papers (KB/WPCC) electrode, a dual gas-diffusion membrane- and mediator-less H_2 /air-breathing biofuel cell was constructed (Figure 3b) which showed maximum power density in the range of $6.1 \text{ mW}\cdot\text{cm}^{-2}$ at 0.72 V [168].

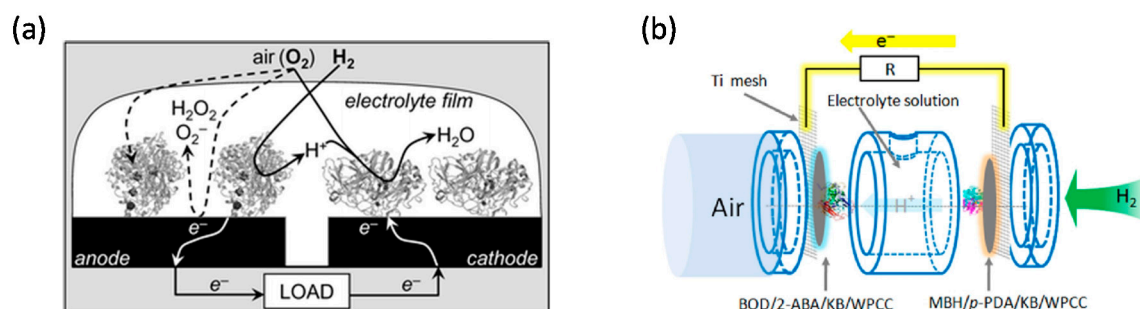


Figure 3. Schematic representations of enzymatic biofuel cells (EBC). (a) EBC comprises of graphite electrodes modified with O_2 -tolerant MBH of *R. metallidurans* CH34 (anode) and fungal laccase (cathode) in aqueous electrolyte exposed to 3% H_2 in air. Reprinted with the permission from ref [166]. Copyright (2006), The Royal Society of Chemistry. (b) A dual gas diffusion membrane-free H_2 /air powered EBC comprises of a [NiFe]-MBH (anode) and a bilirubin oxidase (cathode). Reprinted with the permission from ref [168]. Copyright (2016), Elsevier B.V.

The O_2 -reduction biocathodes for EBC are usually based on multi-copper oxidases like bilirubin oxidase or laccase which can reduce O_2 almost without overpotential [169]. Among the membrane proteins, cytochrome *c* oxidase has been studied as O_2 reduction catalyst. Katz and Willner assembled a membrane-less glucose/ O_2 biofuel cell with cytochrome *c*/cytochrome *c* oxidase as O_2 reducing cathode [170]. The cytochrome *c* was assembled on a maleimide modified gold electrode through a cysteine residue to link cytochrome *c* oxidase. In a follow-up work, the authors developed an electroswitchable and tunable biofuel cell. In this case, the cathode was modified with poly(acrylic acid) loaded with Cu^{2+} to covalently attach cytochrome *c* and link the latter to cytochrome *c* oxidase [171]. Although cytochrome *c* was able mediated electron transfer to cytochrome *c* oxidase for O_2 reduction, only an OCV of 0.12 V was obtained, likely limited by the redox potential of cytochrome *c* ($\sim -0.25 \text{ V}$ vs. SHE), which is much lower than that of $\text{H}_2\text{O}/\text{O}_2$ (0.82 V vs. SHE at pH 7). Although cytochrome *c* oxidase is not commonly used for O_2 reducing cathode in biofuel cell, the recent work with gold NPs by the group of Hellwig has shown renewed possibilities for cytochrome *c* oxidase as catalyst (see Section 3.3). Recently, Wang et al. [172] reported that cytochrome *c* oxidase from acidophilic bacterium *Acidithiobacillus ferrooxidans* can reduce O_2 at exceptionally high electrode potentials ($+700$ to $+540 \text{ mV}$ vs. NHE). The low overpotential for O_2 reduction of this cytochrome *c* oxidase makes it an attractive biocatalyst as cathode of biofuel cells in the future.

Besides the use of H_2 as fuel for EBC, formate is also a valuable feedstock for biofuel cells because its redox potential is similar to H_2/H^+ . The Kano group reported a mediated electron transfer type formate/ O_2 biofuel cell by coupling formate dehydrogenase modified bioanode with BOD modified biocathode [173]. In nature, some formate dehydrogenases can catalyse the inverse reaction to reduce CO_2 to formate [174]. However, to the best of our knowledge, the research in this field has been conducted only on soluble formate dehydrogenases. The ability of CO_2 reduction and the applications of membrane-bound formate dehydrogenase need to be further explored.

Respiratory nitrate reductase (Nar) catalyses NO_3^- reduction to NO_2^- , this is an essential step to produce NH_3 . Today there is no enzyme known to reduce NO_3^- to NH_3 directly [175]. DET with nitrate reductase has been shown to support the electrochemical reduction of NO_3^- to NO_2^- [34,35]. A full reduction of NO_3^- to NH_3 was demonstrated by a cascade electrocatalysis process which combined nitrate reductase and noble metal catalyst to reduce NO_2^- to NH_3 [58].

5.2. Biophotoelectrocatalysis (PEC)

Biophotoelectrodes fabricated on planar carbon or SAM-modified metal electrode usually show low photocurrent density which limits their applications in bioelectrocatalysis. However, the development of redox polymer electrodes, layer-by-layer assembly and 3D architectures has enhanced the performance of biophotoelectrodes [176,177]. PSII is the only natural protein able to catalyse the photooxidation of water. The electron flow can be blocked by herbicide compounds since they bind to the terminal plastoquinone Q_B of PSII. This inhibition effect can be exploited for designing PSII light-driven biosensor to detect herbicides [178]. A similar approach to detect herbicides was taken with purple bacteria RCs [179].

As water oxidation biophotocatalyst, PSII attracts more attention for solar energy conversion to generate electricity or fuels. As mentioned above, PSII photoanodes have been connected to PSI photocathodes (both in Os redox polymers) to mimic natural photosynthesis Z-scheme for solar-to-electricity generation [62,63]. In a similar approach using a benzoquinone redox polymer, a PSII photoanode (O_2 evolution) has been connected to a bilirubin oxidase cathode for O_2 reduction [180]. Recently, PSII was integrated together with PbS quantum dots within a TiO_2 inverse opal electrode to perform H_2O photooxidation. This was combined with an inverse opal antimony-doped tin oxide (ATO) cathode modified with bilirubin oxidase to catalyse oxygen reduction. This system achieved a high open-circuit voltage of about 1V under illumination (Figure 4a,b) [181].

A full water splitting process can be realised by combining a PSII photoanode with a cathode modified with hydrogenases. In contrast to EBCs (Section 5.1), water-soluble hydrogenases (typically [FeFe] hydrogenases, but also [NiFe] hydrogenases; H₂ases) are most commonly used for water splitting systems. When combining PSII and H₂ases, there is an energy gap between the terminal electron acceptor Q_B within PSII and one of the FeS cluster within H₂ase. A biophotoelectrochemical cell with a PSII photoanode and a H₂ase cathode thus requires an applied bias voltage of 0.8 V to drive H_2O splitting [93]. This was improved by wiring H₂ase and p-Si on an inverse opal TiO_2 photocathode, lowering the required applied bias voltage to 0.4 V for H_2O splitting [182]. Finally, by integrating PSII on a diketopyrrolopyrrole dye-sensitised TiO_2 photoanode and connecting it with a H₂ase cathode, a bias-free photoelectrochemical cell for H_2O splitting was developed by the group of Reisner [183]. Coupling a dye-sensitised PSII photoanode with a W-dependent formate dehydrogenase (FDH) cathode, a biophotoelectrochemical cell was constructed for CO_2 reduction at a small bias voltage of 0.3 V (Figure 4c,d) [184]. The latter study showed the possibility for rational design of biophotoelectrochemical cells for value-added chemicals generation beyond H_2 .

Unlike PSII, PSI does not directly catalyse technologically valuable reactions such as water oxidation. However, photoexcitation of PSI provides the reductive potential to drive reactions with other catalysts, such as Pt and H₂ase [185]. Recent studies show that it is possible to drive H_2 production from light with PSI and H₂ase by electrode design. Photoelectrodes were manufactured in a 'layered' fashion using an Os redox polymer, PSI and, finally, a polymer/H₂ase mix [186]. Photoelectrochemical H_2 production is achieved at an onset potential of +0.38 V vs. SHE. In this study, the PSI was randomly orientated and did not form a compact layer, likely limiting efficiency by charge recombination between the carrier and mediator or electrode. In a more recent study, an anisotropically oriented PSI monolayer was formed using Langmuir-Blodgett deposition [187]. A compact and oriented PSI layer minimises charge recombination and enables unidirectional electron transfer to H₂ase for H_2 evolution. Combining this PSI/H₂ase photocathode with a PSII photoanode created a system able of bias-free light-driven water splitting [187]. Langmuir-Blodgett deposition transfers only a monolayer of PSI and this might limit the performance of the biophotoelectrode as this limits the loading or coverage of PSI.

One of the limitations with biophotoelectrodes is the limited lifetime of the isolated proteins, especially PSII [154]. Light-induced formation of reactive oxygen species can further limit the lifespan of proteins [115]. Another limitation of biophotoelectrodes is that photosynthetic proteins only use a limited range of the solar spectrum which reduces solar conversion efficiency. The absorption spectral range can be enhanced by attaching complementary chromophores to light-harvesting complex

proteins [188]. It also can be improved by integrating biological light-harvesting antenna complexes or organic dyes/synthetic compounds to the RCs [189,190].

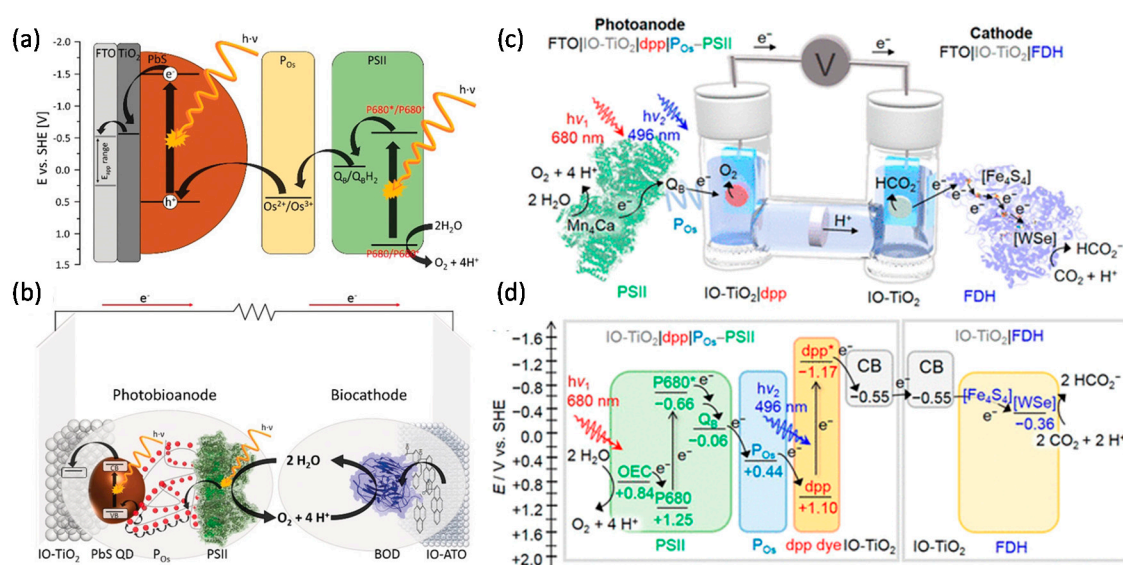


Figure 4. Photoelectrochemical (PEC) cell for electricity or biofuels generation. (a) Schematic of the electron transfer steps and energetic level of the components of the light-driven signal chain composed of TiO₂, PbS QDs, redox polymer (POs), and PSII. (b) A scheme of a PEC cell consisting of an IO-TiO₂|PbS|POs|PSII anode and an IO-ATO|PC|BOD cathode. Reprinted with the permission from ref [181]. Copyright (2019), Wiley. (c) A schematic representation of a semi-artificial photosynthetic tandem PEC cell coupling CO₂ reduction to water oxidation. A blend of POs and PSII adsorbed on a dpp-sensitized photoanode (IO-TiO₂|dpp|POs-PSII) is wired to an IO-TiO₂|FDH cathode. (d) Energy level diagram showing the electron-transfer pathway between PSII, the redox polymer (POs), the dye (dpp), the conduction band (CB) of IO-TiO₂ electrodes, four [Fe₄S₄] clusters, and the [WSe]-active site in FDH. All potentials are reported vs. SHE at pH 6.5. Reprinted with the permission from ref [184]. Copyright (2018), American Chemical Society.

6. Emerging Methods and Future Considerations

6.1. Extending the Lifetime of Membrane Enzymes

A major drawback of enzymes in EBC is their limited active lifetime, which usually ranges from few hours to several days [191]. This applies particularly when membrane enzymes in detergent solutions are used, and functional reconstitution of membrane enzymes into an amphiphilic bilayer, such as liposome or polymersome vesicles, could represent a strategy to extend the enzyme lifetime. Liposomes offer great biocompatibility because they mimic the natural environment of membrane proteins, but they lack chemical and physical long-term stability [192]. Polymersomes offer a more robust amphiphilic polymer environment with increased chemical and physical stability [193,194]. However, this non-native polymeric environment might be limiting the functional incorporation of a wider range of membrane proteins [195]. Recently, hybrid vesicle systems composed of a mixture of lipids and block copolymers, have been developed with the rationale to provide a compromise between the biocompatibility of liposomes and the stability and robustness of polymersomes. In 2016 we showed that hybrid vesicles, composed of biocompatible lipids and stable PBd-PEO copolymer, supported higher activity of reconstituted cytochrome *b*₀₃ than the proteopolymersomes and significantly extended the functional lifetime of the membrane enzyme when compared to standard proteoliposomes [196] (Figure 5). In 2018, we achieved increased stability of cytochrome *b*₀₃ reconstituted in hybrid vesicles up to 500 days [197]. Similarly, recent work from Dimova group showed that functional integration of cytochrome *b*₀₃ oxidase in synthetic membranes made of PDMS-*g*-PEO was capable of lumen

acidification and such reconstituted system showed to increase the active lifetime and resistance to free radicals [198]. In 2017, Otrin et al. [199] demonstrated a similar ability to store gradients by reconstituting cytochrome bo_3 together with an ATP synthase in hybrid vesicles constituted of the same copolymer, PDMS- g -PEO. In 2018, Smirnova et al. presented a method that allowed transfer of a functional membrane protein, cytochrome c oxidase (cytochrome aa_3 or yeast Complex IV), with a disc of its native lipids into pre-formed liposomes of well-defined lipid composition and size using amphipathic styrene maleic acid (SMA) copolymer [200]. This recent advance in using SMA copolymer for membrane enzymes isolation and reconstitution offers the advantage to maintain the native phospholipids environment surrounding the proteins and, moreover, could reduce time and cost for enzyme isolation and reconstitution processes by avoiding detergent mediated extraction [201]. Further research into affordable purification strategies and extending the stability of commercially-relevant membrane enzymes is required for membrane enzymes to find applications in bioelectrocatalysis. An alternative approach would be to omit purification altogether and exploit the regenerative capacity of micro-organisms in microbial electrosynthesis.

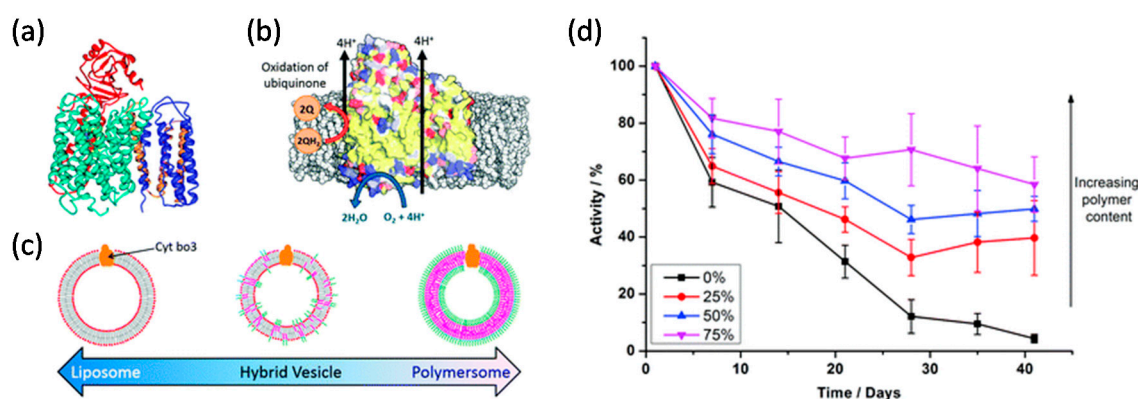


Figure 5. Stability of reconstituted cytochrome bo_3 in hybrid vesicles. (a) Ribbon diagram of cytochrome bo_3 . (b) Schematic representation of cytochrome bo_3 reactions (c) schematic representation of proteo-phospholipid/block copolymer hybrid vesicles. (d) Comparison of cytochrome bo_3 activity in reconstituted hybrid vesicles with increasing polymer content over a period of 41 days. Reprinted with the permission from ref [196]. Copyright (2016), The Royal Society of Chemistry.

6.2. Microbial Electrosynthesis and Whole-Cell Semi-Artificial Photosynthesis

Microorganisms are of great interest for electrochemical applications because of their self-reproduce nature and diverse metabolic processes. The possibility to use directly the microorganisms overcomes the need to purify and manipulate the proteins. Many microorganisms are exoelectrogens and can communicate with electrodes through extracellular electron transfer (EET), either (1) directly through membrane-bound cytochromes and conductive filaments (nanowires) or (2) via a soluble redox species, such as flavins, either natively secreted by the microorganism or added as a mediator [202].

6.2.1. Microbial Electrosynthesis

Microbial electrosynthesis is an electricity-driven process which generates chemicals using microorganisms as catalysts [203]. To date, the most well-studied exoelectrogens are *Geobacter* spp. and *S. oneidensis* [204]. They are dissimilatory metal-reducing bacteria that can reduce extracellular metal ions (and bulk electrodes) as part of their anaerobic respiration. These electron transfer steps can be reversed to gain electron from electrode for reductive synthesis, some catalysed by membrane enzymes in the microorganisms (Figure 6) [205,206]. It has been shown that *Geobacter* spp. can reduce nitrate to nitrite [207], fumarate to succinate [207] and proton to hydrogen [208] using electrode as the electron donor. *S. oneidensis* was also shown to electrocatalytically reduce fumarate to succinate [209]. It also has been reported that *S. oneidensis* can catalyse CO_2 reduction into formic acid with electron input from

the cathode [210]. The cathodic CO₂ reduction in *S. oneidensis* is associated with the electron uptake through outer-membrane c-type cytochromes [211]. The efficiency of the microbial electrosynthesis is mainly limited by the EET. With the genetic engineering of the microorganisms, the EET efficiency can be improved [212–214]. Advances in synthetic biology allow the rational design of non-natural functions in order to increase the diversity of products obtainable from microbial electrosynthesis [215]. For instance, by engineering genes for an ATP-dependent citrate lyase into *Geobacter sulfurreducens*, the microorganism is able to fix CO₂ through a reverse TCA cycle using an electrode as electron donor [216]. A genetically engineered *S. oneidensis* with heterologous Ehrlich pathway genes was shown to produce isobutanol by supplying electricity [217]. It has been demonstrated that *S. oneidensis* can use electrons supplied by an electrode to reduce O₂. This study also showed that the cathodic reaction can reduce NAD⁺ via proton-pumping NADH oxidase complex I [218]. With addition of a light-driven proton pump (proteorhodopsin) in the *S. oneidensis* to generate proton-motive force, the electron transferred from cathode to quinone pool can be used to reduce NAD⁺ to NADH by native NADH dehydrogenases. This was demonstrated by the reduction of acetoin to 2,3-butanediol via a heterologous butanediol dehydrogenase (Bdh) which is a NADH-dependent enzyme [219].

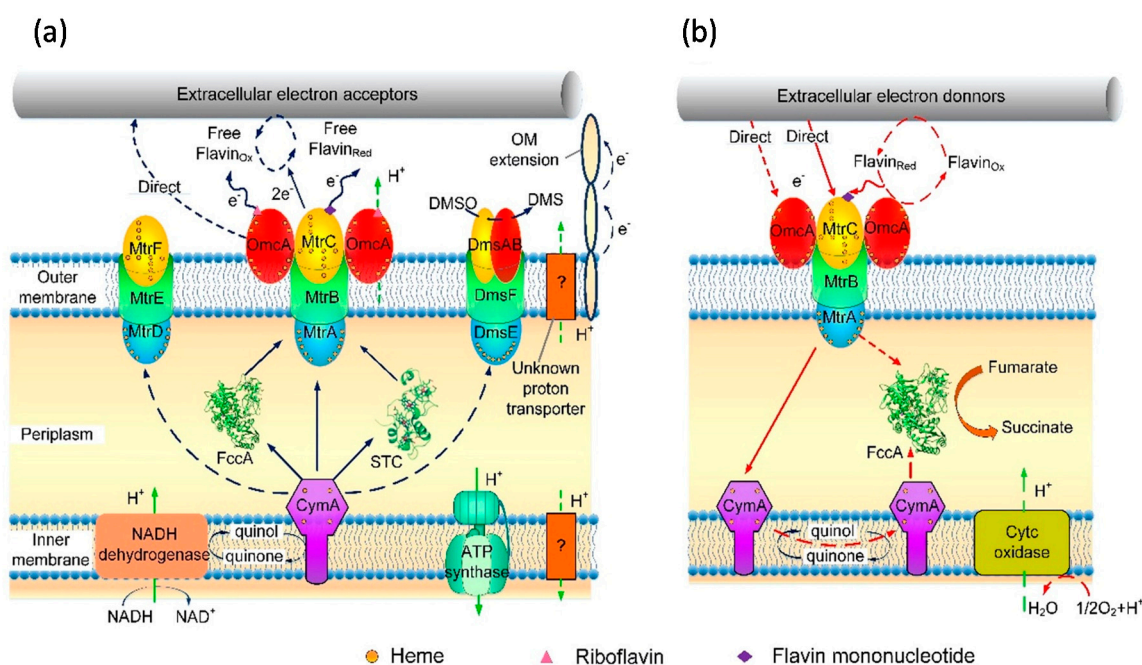


Figure 6. Conceptual model of the bidirectional EET pathways in *S. oneidensis* MR-1. The solid arrows indicate the verified electron flow path, and the dashed arrows indicate the possible electron flow. The blue arrows indicate the outward EET pathway, the red arrows indicate the inward EET pathway, and the green arrows indicate the H⁺ flow pathway. (a) The outward EET toward extracellular acceptors utilizes the metal-reducing (Mtr) pathway. (b) The inward EET toward intracellular terminal reductase involves MtrCBA complex, periplasmic FccA, and inner membrane CymA. The cycle of oxidation (Ox) and reduction (Red) states of self-secreted flavins mediated both outward and inward EET. DMSO, dimethyl sulphoxide; Omc, outer-membrane cytochrome. Reprinted with the permission from ref [220]. Copyright (2020), Taylor & Francis.

6.2.2. Whole-Cell Based Semi-Artificial Photosynthesis

Semi-artificial photosynthesis has attracted great attention for harvesting solar energy for electricity or chemical generation [5]. Instead of isolated photosynthetic proteins (e.g., PSII), photosynthetic microorganisms such as algae [221], cyanobacteria [222–225] and purple bacteria [226], or extracted organelles such as thylakoids [227] have been studied for biophotoelectrochemical systems. The development of 3D structured electrodes increased the loading capacity which enhances

photocurrents [228]. However, low EET rates still limit the efficiency of these photoelectrodes. It has been shown that redox polymers can improve electron transfer kinetics between microorganisms and electrode [221,226]. Furthermore improvement in EET kinetics and new electrode designs for accommodating microorganisms are required to boost the performance of photoelectrochemical devices that are based on photosynthetic microorganisms [111].

An emerging direction in the semi-artificial photosynthesis is to interface synthetic light-harvesting materials with non-photosynthetic microorganisms for value-added chemicals [229,230]. As a model microorganism, *S. oneidensis* has been widely studied for integration with artificial light-harvesting materials for solar-driven microbial synthesis. The transmembrane cytochrome MtrCAB, helped by OmcA located on the outside of the membrane, are known to transfer electrons between the interior of the cell and extracellular materials (Figure 6) [231,232]. In the presence of a sacrificial electron donor, MtrC and OmcA can be photoreduced by water-soluble photosensitisers including eosin Y, fluorescein, proflavine, flavin, and adenine dinucleotide, riboflavin and flavin mononucleotide [233]. In an in vitro approach, it was showed that dye-sensitised TiO₂ nanoparticles can photoreduce MtrC or OmcA, either in solution or on an electrode surface [233–235] and it might be possible to extend this process to reductive photosynthesis in *S. oneidensis* [236]. To provide a proof-of-concept, we recently reconstituted MtrCAB into proteoliposomes encapsulating a redox dye, Reactive Red 120 (RR120), which can be reductively bleached. Using light-harvesting nanoparticles including dye-sensitised TiO₂ nanoparticles, amorphous carbon dots and nitrogen doped graphitic carbon dots, we observed RR120 reductive decomposition inside the lumen of the MtrCAB proteoliposomes, confirming that electrons were transferred from the nanoparticles via transmembrane MtrCAB complex into the liposome lumen [237]. These results show that the rational design of light-harvesting nanoparticles and protein hybrids can lead to the development of semi-artificial photosynthetic systems for solar fuels synthesis.

7. Conclusions

Membrane proteins play an important role for biofuel conversion and photosynthesis, and the catalytic and electron transfer ability of the membrane proteins makes them attractive for applications in bioelectrocatalysis. Recent developments in bioelectrochemistry have provided the means to control and improve electron transfer rate between immobilised proteins and electrodes, stabilising the activity of immobilised enzymes. High surface areas of so-called 3D electrodes are able to increase the protein loading, which is desired for bioelectrocatalysis. Despite these enhanced performances, there is still the need to further optimise this technology for practical use in bioelectrocatalysis devices, especially for membrane enzymes. Combining several immobilisation strategies would provide possible solutions. Advances in characterisation techniques enable detailed characterisation of the structure of the electrode, the electron transfer process, catalytic activity and protein structure, which in turn provides an in-depth understanding of the catalytic reaction mechanism, aiding the rational design of the electrode interface for bioelectrocatalysis. Membrane proteins are known to be difficult to study and manipulate due to their amphiphilic nature. Preserving their stability and functionality is crucial for successful application of this technology. Recently developed redox polymers and hybrid vesicles, composed of lipids and block copolymers, are promising platforms to stabilise membrane proteins on the electrode surface. Using exoelectrogenic microorganisms for electrosynthesis and semi-artificial photosynthesis is an encouraging research direction, which will simplify time and cost related with protein purification processes. The ability of microorganisms to regenerate and self-replicate (at an energy cost), also removes the need to stabilise the biocatalyst. With synthetic biology, the microorganisms can be further engineered for diverse biofuel and chemical synthesis. However, the extracellular electron transfer kinetics might still be limiting the efficiency of the whole-cell based systems, especially when organisms are used that have not been optimised by evolution for extracellular electron transfer.

Funding: This research was funded by the Biotechnology and Biological Sciences Research Council (BBSRC), grant numbers BB/T000546/1 and BB/S000704/1.

Conflicts of Interest: The authors declare no conflict of interest.

References

1. von Heijne, G. Membrane-protein topology. *Nat. Rev. Mol. Cell Biol.* **2006**, *7*, 909–918. [[CrossRef](#)] [[PubMed](#)]
2. Hedin, L.E.; Illergård, K.; Elofsson, A. An introduction to membrane proteins. *J. Proteome Res.* **2011**, *10*, 3324–3331. [[CrossRef](#)] [[PubMed](#)]
3. Tan, S.; Tan, H.T.; Chung, M.C.M. Membrane proteins and membrane proteomics. *Proteomics* **2008**, *8*, 3924–3932. [[CrossRef](#)] [[PubMed](#)]
4. Kumar, G.; Kim, S.-H.; Lay, C.-H.; Ponnusamy, V.K. Recent developments on alternative fuels, energy and environment for sustainability. *Bioresour. Technol.* **2020**, *317*, 124010. [[CrossRef](#)] [[PubMed](#)]
5. Kornienko, N.; Zhang, J.Z.; Sakimoto, K.K.; Yang, P.; Reisner, E. Interfacing nature’s catalytic machinery with synthetic materials for semi-artificial photosynthesis. *Nat. Nanotechnol.* **2018**, *13*, 890–899. [[CrossRef](#)]
6. Vignais, P.M.; Billoud, B.; Meyer, J. Classification and phylogeny of hydrogenases. *FEMS Microbiol. Rev.* **2001**, *25*, 455–501. [[CrossRef](#)]
7. Shima, S.; Pilak, O.; Vogt, S.; Schick, M.; Stagni, M.S.; Meyer-Klaucke, W.; Warkentin, E.; Thauer, R.K.; Ermler, U. The crystal structure of Fe-hydrogenase reveals the geometry of the active site. *Science* **2008**, *321*, 572–575. [[CrossRef](#)]
8. Fritsch, J.; Lenz, O.; Friedrich, B. Structure, function and biosynthesis of O₂-tolerant hydrogenases. *Nat. Rev. Microbiol.* **2013**, *11*, 106–114. [[CrossRef](#)]
9. Sousa, F.L.; Alves, R.J.; Ribeiro, M.A.; Pereira-Leal, J.B.; Teixeira, M.; Pereira, M.M. The superfamily of heme-copper oxygen reductases: Types and evolutionary considerations. *Biochim. Biophys. Acta Bioenerg.* **2012**, *1817*, 629–637. [[CrossRef](#)]
10. Borisov, V.B.; Gennis, R.B.; Hemp, J.; Verkhovsky, M.I. The cytochrome *bd* respiratory oxygen reductases. *Biochim. Biophys. Acta Bioenerg.* **2011**, *1807*, 1398–1413. [[CrossRef](#)]
11. Vanlerberghe, G.C. Alternative oxidase: A mitochondrial respiratory pathway to maintain metabolic and signaling homeostasis during abiotic and biotic stress in plants. *Int. J. Mol. Sci.* **2013**, *14*, 6805–6847. [[CrossRef](#)] [[PubMed](#)]
12. García-Horsman, J.A.; Barquera, B.; Rumbley, J.; Ma, J.; Gennis, R.B. The superfamily of heme-copper respiratory oxidases. *J. Bacteriol.* **1994**, *176*, 5587–5600. [[CrossRef](#)] [[PubMed](#)]
13. Safarian, S.; Hahn, A.; Mills, D.J.; Radloff, M.; Eisinger, M.L.; Nikolaev, A.; Meier-Credo, J.; Melin, F.; Miyoshi, H.; Gennis, R.B.; et al. Active site rearrangement and structural divergence in prokaryotic respiratory oxidases. *Science* **2019**, *366*, 100–104. [[CrossRef](#)] [[PubMed](#)]
14. Moreno-Vivián, C.; Cabello, P.; Martínez-Luque, M.; Blasco, R.; Castillo, F. Prokaryotic nitrate reduction: Molecular properties and functional distinction among bacterial nitrate reductases. *J. Bacteriol.* **1999**, *181*, 6573–6584. [[CrossRef](#)] [[PubMed](#)]
15. Berks, B.C.; Ferguson, S.J.; Moir, J.W.B.; Richardson, D.J. Enzymes and associated electron transport systems that catalyse the respiratory reduction of nitrogen oxides and oxyanions. *Biochim. Biophys. Acta Bioenerg.* **1995**, *1232*, 97–173. [[CrossRef](#)]
16. Bertero, M.G.; Rothery, R.A.; Palak, M.; Hou, C.; Lim, D.; Blasco, F.; Weiner, J.H.; Strynadka, N.C.J. Insights into the respiratory electron transfer pathway from the structure of nitrate reductase A. *Nat. Struct. Biol.* **2003**, *10*, 681–687. [[CrossRef](#)]
17. Nelson, N.; Ben-Shem, A. The complex architecture of oxygenic photosynthesis. *Nat. Rev. Mol. Cell Biol.* **2004**, *5*, 971–982. [[CrossRef](#)]
18. Gao, J.; Wang, H.; Yuan, Q.; Feng, Y. Structure and Function of the Photosystem Supercomplexes. *Front. Plant. Sci.* **2018**, *9*, 357. [[CrossRef](#)]
19. Hu, X.; Damjanović, A.; Ritz, T.; Schulten, K. Architecture and mechanism of the light-harvesting apparatus of purple bacteria. *Proc. Natl. Acad. Sci. USA* **1998**, *95*, 5935–5941. [[CrossRef](#)]
20. Bahatyrova, S.; Frese, R.N.; Siebert, C.A.; Olsen, J.D.; van der Werf, K.O.; van Grondelle, R.; Niederman, R.A.; Bullough, P.A.; Otto, C.; Hunter, C.N. The native architecture of a photosynthetic membrane. *Nature* **2004**, *430*, 1058–1062. [[CrossRef](#)]

21. Mirkovic, T.; Ostroumov, E.E.; Anna, J.M.; van Grondelle, R.; Govindjee; Scholes, G.D. Light Absorption and Energy Transfer in the Antenna Complexes of Photosynthetic Organisms. *Chem. Rev.* **2017**, *117*, 249–293. [[CrossRef](#)] [[PubMed](#)]
22. Plumeré, N.; Nowaczyk, M.M. Biophotoelectrochemistry of Photosynthetic Proteins. In *Biophotoelectrochemistry: From Bioelectrochemistry to Biophotovoltaics*; Jeuken, L., Ed.; Springer: Cham, Switzerland, 2016; Volume 158, pp. 111–136.
23. Yehezkeili, O.; Tel-Vered, R.; Michaeli, D.; Willner, I.; Nechushtai, R. Photosynthetic reaction center-functionalized electrodes for photo-bioelectrochemical cells. *Photosynth. Res.* **2014**, *120*, 71–85. [[CrossRef](#)] [[PubMed](#)]
24. Chen, H.; Simoska, O.; Lim, K.; Grattieri, M.; Yuan, M.; Dong, F.; Lee, Y.S.; Beaver, K.; Weliwatte, S.; Gaffney, E.M.; et al. Fundamentals, Applications, and Future Directions of Bioelectrocatalysis. *Chem. Rev.* **2020**. [[CrossRef](#)] [[PubMed](#)]
25. Carpenter, E.P.; Beis, K.; Cameron, A.D.; Iwata, S. Overcoming the challenges of membrane protein crystallography. *Curr. Opin. Struct. Biol.* **2008**, *18*, 581–586. [[CrossRef](#)]
26. Seddon, A.M.; Curnow, P.; Booth, P.J. Membrane proteins, lipids and detergents: Not just a soap opera. *Biochim. Biophys. Acta* **2004**, *1666*, 105–117. [[CrossRef](#)]
27. Palazzo, G. Colloidal aspects of photosynthetic membrane proteins. *Curr. Opin. Colloid Interface Sci.* **2006**, *11*, 65–73. [[CrossRef](#)]
28. Rawlings, A.E. Membrane proteins: Always an insoluble problem? *Biochem. Soc. Trans.* **2016**, *44*, 790–795. [[CrossRef](#)]
29. Gillam, E.M.J. Engineering cytochrome P450 enzymes. *Chem. Res. Toxicol.* **2008**, *21*, 220–231. [[CrossRef](#)]
30. Hunte, C.; Richers, S. Lipids and membrane protein structures. *Curr. Opin. Struct. Biol.* **2008**, *18*, 406–411. [[CrossRef](#)]
31. Mazurenko, I.; Hitaishi, V.P.; Lojou, E. Recent advances in surface chemistry of electrodes to promote direct enzymatic bioelectrocatalysis. *Curr. Opin. Electrochem.* **2020**, *19*, 113–121. [[CrossRef](#)]
32. Yates, N.D.J.; Fascione, M.A.; Parkin, A. Methodologies for “Wiring” Redox Proteins/Enzymes to Electrode Surfaces. *Chem. Eur. J.* **2018**, *24*, 12164–12182. [[CrossRef](#)] [[PubMed](#)]
33. Sucheta, A.; Ackrell, B.A.; Cochran, B.; Armstrong, F.A. Diode-like behaviour of a mitochondrial electron-transport enzyme. *Nature* **1992**, *356*, 361–362. [[CrossRef](#)] [[PubMed](#)]
34. Anderson, L.J.; Richardson, D.J.; Butt, J.N. Catalytic protein film voltammetry from a respiratory nitrate reductase provides evidence for complex electrochemical modulation of enzyme activity. *Biochemistry* **2001**, *40*, 11294–11307. [[CrossRef](#)] [[PubMed](#)]
35. Elliott, S.J.; Hoke, K.R.; Heffron, K.; Palak, M.; Rothery, R.A.; Weiner, J.H.; Armstrong, F.A. Voltammetric studies of the catalytic mechanism of the respiratory nitrate reductase from *Escherichia coli*: How nitrate reduction and inhibition depend on the oxidation state of the active site. *Biochemistry* **2004**, *43*, 799–807. [[CrossRef](#)]
36. den Hollander, M.-J.; Magis, J.G.; Fuchsenberger, P.; Aartsma, T.J.; Jones, M.R.; Frese, R.N. Enhanced photocurrent generation by photosynthetic bacterial reaction centers through molecular relays, light-harvesting complexes, and direct protein-gold interactions. *Langmuir* **2011**, *27*, 10282–10294. [[CrossRef](#)]
37. Kamran, M.; Delgado, J.D.; Friebe, V.; Aartsma, T.J.; Frese, R.N. Photosynthetic protein complexes as bio-photovoltaic building blocks retaining a high internal quantum efficiency. *Biomacromolecules* **2014**, *15*, 2833–2838. [[CrossRef](#)]
38. Yasuda, Y.; Sugino, H.; Toyotama, H.; Hirata, Y.; Hara, M.; Miyake, J. Control of protein orientation in molecular photoelectric devices using Langmuir–Blodgett films of photosynthetic reaction centers from *Rhodospseudomonas viridis*. *Bioelectrochem. Bioenerg.* **1994**, *34*, 135–139. [[CrossRef](#)]
39. Uphaus, R.A.; Fang, J.Y.; Picorel, R.; Chumanov, G.; Wang, J.Y.; Cotton, T.M.; Seibert, M. Langmuir–Blodgett and X-ray diffraction studies of isolated photosystem II reaction centers in monolayers and multilayers: Physical dimensions of the complex. *Photochem. Photobiol.* **1997**, *65*, 673–679. [[CrossRef](#)]
40. Kernen, P.; Gruszecki, W.I.; Matuła, M.; Wagner, P.; Ziegler, U.; Krupa, Z. Light-harvesting complex II in monocomponent and mixed lipid-protein monolayers. *Biochim. Biophys. Acta Biomembr.* **1998**, *1373*, 289–298. [[CrossRef](#)]
41. Pepe, I.M.; Nicolini, C. Langmuir–Blodgett films of photosensitive proteins. *J. Photochem. Photobiol. B* **1996**, *33*, 191–200. [[CrossRef](#)]

42. Ko, B.S.; Babcock, B.; Jennings, G.K.; Tilden, S.G.; Peterson, R.R.; Cliffel, D.; Greenbaum, E. Effect of surface composition on the adsorption of photosystem I onto alkanethiolate self-assembled monolayers on gold. *Langmuir* **2004**, *20*, 4033–4038. [[CrossRef](#)] [[PubMed](#)]
43. Lee, I.; Lee, J.W.; Greenbaum, E. Biomolecular Electronics: Vectorial Arrays of Photosynthetic Reaction Centers. *Phys. Rev. Lett.* **1997**, *79*, 3294–3297. [[CrossRef](#)]
44. Trammell, S.A.; Wang, L.; Zullo, J.M.; Shashidhar, R.; Lebedev, N. Orientated binding of photosynthetic reaction centers on gold using Ni-NTA self-assembled monolayers. *Biosens. Bioelectron.* **2004**, *19*, 1649–1655. [[CrossRef](#)] [[PubMed](#)]
45. Nakamura, C.; Hasegawa, M.; Yasuda, Y.; Miyake, J. Self-Assembling Photosynthetic Reaction Centers on Electrodes for Current Generation. In *Twenty-First Symposium on Biotechnology for Fuels and Chemicals*; Finkelstein, M., Davison, B.H., Eds.; Humana Press: Totowa, NJ, USA, 2000; Volume 84–86, pp. 401–408.
46. Maly, J.; Krejci, J.; Ilie, M.; Jakubka, L.; Masojidek, J.; Pilloton, R.; Sameh, K.; Steffan, P.; Stryhal, Z.; Sugiura, M. Monolayers of photosystem II on gold electrodes with enhanced sensor response-effect of porosity and protein layer arrangement. *Anal. Bioanal. Chem.* **2005**, *381*, 1558–1567. [[CrossRef](#)]
47. Faulkner, C.J.; Lees, S.; Ciesielski, P.N.; Cliffel, D.E.; Jennings, G.K. Rapid assembly of photosystem I monolayers on gold electrodes. *Langmuir* **2008**, *24*, 8409–8412. [[CrossRef](#)]
48. Friebe, V.M.; Millo, D.; Swainsbury, D.J.K.; Jones, M.R.; Frese, R.N. Cytochrome *c* Provides an Electron-Funneling Antenna for Efficient Photocurrent Generation in a Reaction Center Biophotocathode. *ACS Appl. Mater. Interfaces* **2017**, *9*, 23379–23388. [[CrossRef](#)]
49. Badura, A.; Kothe, T.; Schuhmann, W.; Rögner, M. Wiring photosynthetic enzymes to electrodes. *Energy Environ. Sci.* **2011**, *4*, 3263. [[CrossRef](#)]
50. Xiao, Y.; Patolsky, F.; Katz, E.; Hainfeld, J.F.; Willner, I. “Plugging into Enzymes”: Nanowiring of redox enzymes by a gold nanoparticle. *Science* **2003**, *299*, 1877–1881. [[CrossRef](#)]
51. Fournier, E.; Nikolaev, A.; Nasiri, H.R.; Hoeser, J.; Friedrich, T.; Hellwig, P.; Melin, F. Creation of a gold nanoparticle based electrochemical assay for the detection of inhibitors of bacterial cytochrome *bd* oxidases. *Bioelectrochemistry* **2016**, *111*, 109–114. [[CrossRef](#)]
52. Meyer, T.; Melin, F.; Richter, O.-M.H.; Ludwig, B.; Kannt, A.; Müller, H.; Michel, H.; Hellwig, P. Electrochemistry suggests proton access from the exit site to the binuclear center in *Paracoccus denitrificans* cytochrome *c* oxidase pathway variants. *FEBS Lett.* **2015**, *589*, 565–568. [[CrossRef](#)]
53. Meyer, T.; Melin, F.; Xie, H.; von der Hocht, I.; Choi, S.K.; Noor, M.R.; Michel, H.; Gennis, R.B.; Soulimane, T.; Hellwig, P. Evidence for distinct electron transfer processes in terminal oxidases from different origin by means of protein film voltammetry. *J. Am. Chem. Soc.* **2014**, *136*, 10854–10857. [[CrossRef](#)] [[PubMed](#)]
54. Melin, F.; Meyer, T.; Lankiang, S.; Choi, S.K.; Gennis, R.B.; Blanck, C.; Schmutz, M.; Hellwig, P. Direct electrochemistry of cytochrome *bo*₃ oxidase at a series of gold nanoparticles-modified electrodes. *Electrochem. Commun.* **2013**, *26*, 105–108. [[CrossRef](#)] [[PubMed](#)]
55. Nikolaev, A.; Makarchuk, I.; Thesseling, A.; Hoeser, J.; Friedrich, T.; Melin, F.; Hellwig, P. Stabilization of the Highly Hydrophobic Membrane Protein, Cytochrome *bd* Oxidase, on Metallic Surfaces for Direct Electrochemical Studies. *Molecules* **2020**, *25*, 3240. [[CrossRef](#)]
56. Asadian, E.; Ghalkhani, M.; Shahrokhian, S. Electrochemical sensing based on carbon nanoparticles: A review. *Sens. Actuators B* **2019**, *293*, 183–209. [[CrossRef](#)]
57. Vincent, K.A.; Li, X.; Blanford, C.F.; Belsey, N.A.; Weiner, J.H.; Armstrong, F.A. Enzymatic catalysis on conducting graphite particles. *Nat. Chem. Biol.* **2007**, *3*, 761–762. [[CrossRef](#)]
58. Duca, M.; Weeks, J.R.; Fedor, J.G.; Weiner, J.H.; Vincent, K.A. Combining Noble Metals and Enzymes for Relay Cascade Electrocatalysis of Nitrate Reduction to Ammonia at Neutral pH. *ChemElectroChem* **2015**, *2*, 1086–1089. [[CrossRef](#)]
59. Ruff, A. Redox polymers in bioelectrochemistry: Common playgrounds and novel concepts. *Curr. Opin. Electrochem.* **2017**, *5*, 66–73. [[CrossRef](#)]
60. Badura, A.; Guschin, D.; Kothe, T.; Kopczak, M.J.; Schuhmann, W.; Rögner, M. Photocurrent generation by photosystem 1 integrated in crosslinked redox hydrogels. *Energy Environ. Sci.* **2011**, *4*, 2435. [[CrossRef](#)]
61. Badura, A.; Guschin, D.; Esper, B.; Kothe, T.; Neugebauer, S.; Schuhmann, W.; Rögner, M. Photo-Induced Electron Transfer Between Photosystem 2 via Cross-linked Redox Hydrogels. *Electroanalysis* **2008**, *20*, 1043–1047. [[CrossRef](#)]

62. Kothe, T.; Plumeré, N.; Badura, A.; Nowaczyk, M.M.; Guschin, D.A.; Rögner, M.; Schuhmann, W. Combination of a photosystem 1-based photocathode and a photosystem 2-based photoanode to a Z-scheme mimic for biophotovoltaic applications. *Angew. Chem. Int. Ed.* **2013**, *52*, 14233–14236. [[CrossRef](#)]
63. Hartmann, V.; Kothe, T.; Pöller, S.; El-Mohsnawy, E.; Nowaczyk, M.M.; Plumeré, N.; Schuhmann, W.; Rögner, M. Redox hydrogels with adjusted redox potential for improved efficiency in Z-scheme inspired biophotovoltaic cells. *Phys. Chem. Chem. Phys.* **2014**, *16*, 11936–11941. [[CrossRef](#)] [[PubMed](#)]
64. Kothe, T.; Pöller, S.; Zhao, F.; Fortgang, P.; Rögner, M.; Schuhmann, W.; Plumeré, N. Engineered electron-transfer chain in photosystem 1 based photocathodes outperforms electron-transfer rates in natural photosynthesis. *Chem. Eur. J.* **2014**, *20*, 11029–11034. [[CrossRef](#)] [[PubMed](#)]
65. Laftoglou, T.; Jeuken, L.J.C. Supramolecular electrode assemblies for bioelectrochemistry. *Chem. Commun.* **2017**, *53*, 3801–3809. [[CrossRef](#)] [[PubMed](#)]
66. Jeuken, L.J.C. Electrodes for integral membrane enzymes. *Nat. Prod. Rep.* **2009**, *26*, 1234–1240. [[CrossRef](#)] [[PubMed](#)]
67. Alvarez-Malmagro, J.; García-Molina, G.; López De Lacey, A. Electrochemical Biosensors Based on Membrane-Bound Enzymes in Biomimetic Configurations. *Sensors* **2020**, *20*, 3393. [[CrossRef](#)] [[PubMed](#)]
68. Burgess, J.D.; Rhoten, M.C.; Hawkrigde, F.M. Cytochrome *c* Oxidase Immobilized in Stable Supported Lipid Bilayer Membranes. *Langmuir* **1998**, *14*, 2467–2475. [[CrossRef](#)]
69. Rhoten, M.C.; Hawkrigde, F.M.; Wilczek, J. The reaction of cytochrome *c* with bovine and *Bacillus stearothermophilus* cytochrome *c* oxidase immobilized in electrode-supported lipid bilayer membranes. *J. Electroanal. Chem.* **2002**, *535*, 97–106. [[CrossRef](#)]
70. Kong, J.; Lu, Z.; Lvov, Y.M.; Desamero, R.Z.B.; Frank, H.A.; Rusling, J.F. Direct Electrochemistry of Cofactor Redox Sites in a Bacterial Photosynthetic Reaction Center Protein. *J. Am. Chem. Soc.* **1998**, *120*, 7371–7372. [[CrossRef](#)]
71. Munge, B.; Pendon, Z.; Frank, H.A.; Rusling, J.F. Electrochemical reactions of redox cofactors in *Rhodobacter sphaeroides* reaction center proteins in lipid films. *Bioelectrochemistry* **2001**, *54*, 145–150. [[CrossRef](#)]
72. Munge, B.; Das, S.K.; Ilagan, R.; Pendon, Z.; Yang, J.; Frank, H.A.; Rusling, J.F. Electron transfer reactions of redox cofactors in spinach photosystem I reaction center protein in lipid films on electrodes. *J. Am. Chem. Soc.* **2003**, *125*, 12457–12463. [[CrossRef](#)]
73. Alcantara, K.; Munge, B.; Pendon, Z.; Frank, H.A.; Rusling, J.F. Thin film voltammetry of spinach photosystem II. Proton-gated electron transfer involving the Mn₄ cluster. *J. Am. Chem. Soc.* **2006**, *128*, 14930–14937. [[CrossRef](#)] [[PubMed](#)]
74. Noji, T.; Matsuo, M.; Takeda, N.; Sumino, A.; Kondo, M.; Nango, M.; Itoh, S.; Dewa, T. Lipid-Controlled Stabilization of Charge-Separated States (P⁺Q_B⁻) and Photocurrent Generation Activity of a Light-Harvesting-Reaction Center Core Complex (LH1-RC) from *Rhodospseudomonas palustris*. *J. Phys. Chem. B* **2018**, *122*, 1066–1080. [[CrossRef](#)] [[PubMed](#)]
75. Jeuken, L.J.C.; Connell, S.D.; Henderson, P.J.F.; Gennis, R.B.; Evans, S.D.; Bushby, R.J. Redox enzymes in tethered membranes. *J. Am. Chem. Soc.* **2006**, *128*, 1711–1716. [[CrossRef](#)] [[PubMed](#)]
76. Radu, V.; Frielingsdorf, S.; Evans, S.D.; Lenz, O.; Jeuken, L.J.C. Enhanced oxygen-tolerance of the full heterotrimeric membrane-bound NiFe-hydrogenase of *Ralstonia eutropha*. *J. Am. Chem. Soc.* **2014**, *136*, 8512–8515. [[CrossRef](#)]
77. Pelster, L.N.; Minter, S.D. Mitochondrial Inner Membrane Biomimic for the Investigation of Electron Transport Chain Supercomplex Bioelectrocatalysis. *ACS Catal.* **2016**, *6*, 4995–4999. [[CrossRef](#)]
78. Ataka, K.; Giess, F.; Knoll, W.; Naumann, R.; Haber-Pohlmeier, S.; Richter, B.; Heberle, J. Oriented attachment and membrane reconstitution of His-tagged cytochrome *c* oxidase to a gold electrode: In situ monitoring by surface-enhanced infrared absorption spectroscopy. *J. Am. Chem. Soc.* **2004**, *126*, 16199–16206. [[CrossRef](#)]
79. Ataka, K.; Richter, B.; Heberle, J. Orientational control of the physiological reaction of cytochrome *c* oxidase tethered to a gold electrode. *J. Phys. Chem. B* **2006**, *110*, 9339–9347. [[CrossRef](#)]
80. Friedrich, M.G.; Giebeta, F.; Naumann, R.; Knoll, W.; Ataka, K.; Heberle, J.; Hrabakova, J.; Murgida, D.H.; Hildebrandt, P. Active site structure and redox processes of cytochrome *c* oxidase immobilised in a novel biomimetic lipid membrane on an electrode. *Chem. Commun.* **2004**, 2376–2377. [[CrossRef](#)]
81. Lisdat, F. Trends in the layer-by-layer assembly of redox proteins and enzymes in bioelectrochemistry. *Curr. Opin. Electrochem.* **2017**, *5*, 165–172. [[CrossRef](#)]

82. Stieger, K.R.; Ciornii, D.; Kölsch, A.; Hejazi, M.; Lokstein, H.; Feifel, S.C.; Zouni, A.; Lisdat, F. Engineering of supramolecular photoactive protein architectures: The defined co-assembly of photosystem I and cytochrome *c* using a nanoscaled DNA-matrix. *Nanoscale* **2016**, *8*, 10695–10705. [[CrossRef](#)]
83. Zhang, Y.; LaFountain, A.M.; Magdaong, N.; Fuciman, M.; Allen, J.P.; Frank, H.A.; Rusling, J.F. Thin film voltammetry of wild type and mutant reaction center proteins from photosynthetic bacteria. *J. Phys. Chem. B* **2011**, *115*, 3226–3232. [[CrossRef](#)] [[PubMed](#)]
84. Mallardi, A.; Giustini, M.; Lopez, F.; Dezi, M.; Venturoli, G.; Palazzo, G. Functionality of photosynthetic reaction centers in polyelectrolyte multilayers: Toward an herbicide biosensor. *J. Phys. Chem. B* **2007**, *111*, 3304–3314. [[CrossRef](#)] [[PubMed](#)]
85. Heath, G.R.; Li, M.; Polignano, I.L.; Richens, J.L.; Catucci, G.; O’Shea, P.; Sadeghi, S.J.; Gilardi, G.; Butt, J.N.; Jeuken, L.J.C. Layer-by-Layer Assembly of Supported Lipid Bilayer Poly-L-Lysine Multilayers. *Biomacromolecules* **2016**, *17*, 324–335. [[CrossRef](#)] [[PubMed](#)]
86. Heath, G.R.; Li, M.; Rong, H.; Radu, V.; Frielingsdorf, S.; Lenz, O.; Butt, J.N.; Jeuken, L.J.C. Multilayered Lipid Membrane Stacks for Biocatalysis Using Membrane Enzymes. *Adv. Funct. Mater.* **2017**, *27*, 1606265. [[CrossRef](#)]
87. Sun, H.; Zhu, J.; Baumann, D.; Peng, L.; Xu, Y.; Shakir, I.; Huang, Y.; Duan, X. Hierarchical 3D electrodes for electrochemical energy storage. *Nat. Rev. Mater.* **2019**, *4*, 45–60. [[CrossRef](#)]
88. Friebe, V.M.; Delgado, J.D.; Swainsbury, D.J.K.; Gruber, J.M.; Chanaewa, A.; van Grondelle, R.; von Hauff, E.; Millo, D.; Jones, M.R.; Frese, R.N. Plasmon-Enhanced Photocurrent of Photosynthetic Pigment Proteins on Nanoporous Silver. *Adv. Funct. Mater.* **2016**, *26*, 285–292. [[CrossRef](#)]
89. Ciesielski, P.N.; Scott, A.M.; Faulkner, C.J.; Berron, B.J.; Cliffel, D.E.; Jennings, G.K. Functionalized nanoporous gold leaf electrode films for the immobilization of photosystem I. *ACS Nano* **2008**, *2*, 2465–2472. [[CrossRef](#)]
90. Lu, Y.; Yuan, M.; Liu, Y.; Tu, B.; Xu, C.; Liu, B.; Zhao, D.; Kong, J. Photoelectric performance of bacteria photosynthetic proteins entrapped on tailored mesoporous WO₃-TiO₂ films. *Langmuir* **2005**, *21*, 4071–4076. [[CrossRef](#)]
91. Kato, M.; Cardona, T.; Rutherford, A.W.; Reisner, E. Photoelectrochemical water oxidation with photosystem II integrated in a mesoporous indium-tin oxide electrode. *J. Am. Chem. Soc.* **2012**, *134*, 8332–8335. [[CrossRef](#)]
92. Kato, M.; Cardona, T.; Rutherford, A.W.; Reisner, E. Covalent immobilization of oriented photosystem II on a nanostructured electrode for solar water oxidation. *J. Am. Chem. Soc.* **2013**, *135*, 10610–10613. [[CrossRef](#)]
93. Mersch, D.; Lee, C.-Y.; Zhang, J.Z.; Brinkert, K.; Fontecilla-Camps, J.C.; Rutherford, A.W.; Reisner, E. Wiring of Photosystem II to Hydrogenase for Photoelectrochemical Water Splitting. *J. Am. Chem. Soc.* **2015**, *137*, 8541–8549. [[CrossRef](#)] [[PubMed](#)]
94. Sokol, K.P.; Mersch, D.; Hartmann, V.; Zhang, J.Z.; Nowaczyk, M.M.; Rögner, M.; Ruff, A.; Schuhmann, W.; Plumeré, N.; Reisner, E. Rational wiring of photosystem II to hierarchical indium tin oxide electrodes using redox polymers. *Energy Environ. Sci.* **2016**, *9*, 3698–3709. [[CrossRef](#)]
95. Stieger, K.R.; Feifel, S.C.; Lokstein, H.; Hejazi, M.; Zouni, A.; Lisdat, F. Biohybrid architectures for efficient light-to-current conversion based on photosystem I within scalable 3D mesoporous electrodes. *J. Mater. Chem. A* **2016**, *4*, 17009–17017. [[CrossRef](#)]
96. Wolfe, K.D.; Dervishogullari, D.; Stachurski, C.D.; Passantino, J.M.; Kane Jennings, G.; Cliffel, D.E. Photosystem I Multilayers within Porous Indium Tin Oxide Cathodes Enhance Mediated Electron Transfer. *ChemElectroChem* **2020**, *7*, 596–603. [[CrossRef](#)]
97. Armstrong, F.A.; Butt, J.N.; Sucheta, A. [18] Voltammetric studies of redox-active centers in metalloproteins adsorbed on electrodes. *Methods Enzymol.* **1993**, *227*, 479–500. [[PubMed](#)]
98. Léger, C.; Elliott, S.J.; Hoke, K.R.; Jeuken, L.J.C.; Jones, A.K.; Armstrong, F.A. Enzyme electrokinetics: Using protein film voltammetry to investigate redox enzymes and their mechanisms. *Biochemistry* **2003**, *42*, 8653–8662. [[CrossRef](#)]
99. Armstrong, F.A. Recent developments in dynamic electrochemical studies of adsorbed enzymes and their active sites. *Curr. Opin. Chem. Biol.* **2005**, *9*, 110–117. [[CrossRef](#)]
100. Melin, F.; Hellwig, P. Recent advances in the electrochemistry and spectroelectrochemistry of membrane proteins. *Biol. Chem.* **2013**, *394*, 593–609. [[CrossRef](#)]
101. Vacek, J.; Zatloukalova, M.; Novak, D. Electrochemistry of membrane proteins and protein–lipid assemblies. *Curr. Opin. Electrochem.* **2018**, *12*, 73–80. [[CrossRef](#)]

102. Armstrong, F.A.; Heering, H.A.; Hirst, J. Reaction of complex metalloproteins studied by protein-film voltammetry. *Chem. Soc. Rev.* **1997**, *26*, 169–179. [[CrossRef](#)]
103. Léger, C.; Bertrand, P. Direct electrochemistry of redox enzymes as a tool for mechanistic studies. *Chem. Rev.* **2008**, *108*, 2379–2438. [[CrossRef](#)] [[PubMed](#)]
104. Butt, J.N.; Armstrong, F.A. Voltammetry of Adsorbed Redox Enzymes: Mechanisms in the Potential Dimension. In *Bioinorganic Electrochemistry*; Hammerich, O., Ulstrup, J., Eds.; Springer: Dordrecht, The Netherlands, 2008; Volume 101, pp. 91–128.
105. Fourmond, V.; Léger, C. Protein Electrochemistry: Questions and Answers. In *Biophotoelectrochemistry: From Bioelectrochemistry to Biophotovoltaics*; Jeuken, L., Ed.; Springer: Cham, Switzerland, 2016; Volume 158, pp. 1–41.
106. Fourmond, V.; Léger, C. Modelling the voltammetry of adsorbed enzymes and molecular catalysts. *Curr. Opin. Electrochem.* **2017**, *1*, 110–120. [[CrossRef](#)]
107. Lang, H.; Duschl, C.; Vogel, H. A new class of thiolipids for the attachment of lipid bilayers on gold surfaces. *Langmuir* **1994**, *10*, 197–210. [[CrossRef](#)]
108. Millo, D.; Bonifacio, A.; Moncelli, M.R.; Sergio, V.; Gooijer, C.; van der Zwan, G. Characterization of hybrid bilayer membranes on silver electrodes as biocompatible SERS substrates to study membrane-protein interactions. *Colloids Surf. B* **2010**, *81*, 212–216. [[CrossRef](#)] [[PubMed](#)]
109. Kato, M.; Zhang, J.Z.; Paul, N.; Reisner, E. Protein film photoelectrochemistry of the water oxidation enzyme photosystem II. *Chem. Soc. Rev.* **2014**, *43*, 6485–6497. [[CrossRef](#)] [[PubMed](#)]
110. Kornienko, N.; Ly, K.H.; Robinson, W.E.; Heidary, N.; Zhang, J.Z.; Reisner, E. Advancing Techniques for Investigating the Enzyme-Electrode Interface. *Acc. Chem. Res.* **2019**, *52*, 1439–1448. [[CrossRef](#)] [[PubMed](#)]
111. Zhang, J.Z.; Reisner, E. Advancing photosystem II photoelectrochemistry for semi-artificial photosynthesis. *Nat. Rev. Chem.* **2020**, *4*, 6–21. [[CrossRef](#)]
112. Kornienko, N.; Zhang, J.Z.; Sokol, K.P.; Lamaison, S.; Fantuzzi, A.; van Grondelle, R.; Rutherford, A.W.; Reisner, E. Oxygenic Photoreactivity in Photosystem II Studied by Rotating Ring Disk Electrochemistry. *J. Am. Chem. Soc.* **2018**, *140*, 17923–17931. [[CrossRef](#)]
113. Zhao, F.; Conzuelo, F.; Hartmann, V.; Li, H.; Nowaczyk, M.M.; Plumeré, N.; Rögner, M.; Schuhmann, W. Light Induced H₂ Evolution from a Biophotocathode Based on Photosystem I–Pt Nanoparticles Complexes Integrated in Solvated Redox Polymers Films. *J. Phys. Chem. B* **2015**, *119*, 13726–13731. [[CrossRef](#)]
114. Zhao, F.; Plumeré, N.; Nowaczyk, M.M.; Ruff, A.; Schuhmann, W.; Conzuelo, F. Interrogation of a PS1-Based Photocathode by Means of Scanning Photoelectrochemical Microscopy. *Small* **2017**, *13*, 1604093. [[CrossRef](#)]
115. Zhao, F.; Hardt, S.; Hartmann, V.; Zhang, H.; Nowaczyk, M.M.; Rögner, M.; Plumeré, N.; Schuhmann, W.; Conzuelo, F. Light-induced formation of partially reduced oxygen species limits the lifetime of photosystem 1-based biocathodes. *Nat. Commun.* **2018**, *9*, 1973. [[CrossRef](#)] [[PubMed](#)]
116. Demirel, G.; Usta, H.; Yilmaz, M.; Celik, M.; Alidagi, H.A.; Buyukserin, F. Surface-enhanced Raman spectroscopy (SERS): An adventure from plasmonic metals to organic semiconductors as SERS platforms. *J. Mater. Chem. C* **2018**, *6*, 5314–5335. [[CrossRef](#)]
117. Grytsyk, N.; Boubegtiten-Fezoua, Z.; Javahiraly, N.; Omeis, F.; Devaux, E.; Hellwig, P. Surface-enhanced resonance Raman spectroscopy of heme proteins on a gold grid electrode. *Spectrochim. Acta Part A* **2020**, *230*, 118081. [[CrossRef](#)] [[PubMed](#)]
118. Hrabakova, J.; Ataka, K.; Heberle, J.; Hildebrandt, P.; Murgida, D.H. Long distance electron transfer in cytochrome *c* oxidase immobilised on electrodes. A surface enhanced resonance Raman spectroscopic study. *Phys. Chem. Chem. Phys.* **2006**, *8*, 759–766. [[CrossRef](#)]
119. Sezer, M.; Frielingsdorf, S.; Millo, D.; Heidary, N.; Utesch, T.; Mroginski, M.-A.; Friedrich, B.; Hildebrandt, P.; Zebger, I.; Weidinger, I.M. Role of the HoxZ subunit in the electron transfer pathway of the membrane-bound NiFe-hydrogenase from *Ralstonia eutropha* immobilized on electrodes. *J. Phys. Chem. B* **2011**, *115*, 10368–10374. [[CrossRef](#)]
120. Ataka, K.; Stripp, S.T.; Heberle, J. Surface-enhanced infrared absorption spectroscopy (SEIRAS) to probe monolayers of membrane proteins. *Biochim. Biophys. Acta* **2013**, *1828*, 2283–2293. [[CrossRef](#)]
121. Wiebalck, S.; Kozuch, J.; Forbrig, E.; Tzschucke, C.C.; Jeuken, L.J.C.; Hildebrandt, P. Monitoring the Transmembrane Proton Gradient Generated by Cytochrome *bo*₃ in Tethered Bilayer Lipid Membranes Using SEIRA Spectroscopy. *J. Phys. Chem. B* **2016**, *120*, 2249–2256. [[CrossRef](#)]

122. López-Lorente, Á.I.; Kranz, C. Recent advances in biomolecular vibrational spectroelectrochemistry. *Curr. Opin. Electrochem.* **2017**, *5*, 106–113. [[CrossRef](#)]
123. Zhai, Y.; Zhu, Z.; Zhou, S.; Zhu, C.; Dong, S. Recent advances in spectroelectrochemistry. *Nanoscale* **2018**, *10*, 3089–3111. [[CrossRef](#)]
124. Melin, F.; Hellwig, P. Redox Properties of the Membrane Proteins from the Respiratory Chain. *Chem. Rev.* **2020**, *120*, 10244–10297. [[CrossRef](#)]
125. Białek, R.; Friebe, V.; Ruff, A.; Jones, M.R.; Frese, R.; Gibasiewicz, K. *In situ* spectroelectrochemical investigation of a biophotocathode based on photoreaction centers embedded in a redox hydrogel. *Electrochim. Acta* **2020**, *330*, 135190. [[CrossRef](#)]
126. Ash, P.A.; Vincent, K.A. Spectroscopic analysis of immobilised redox enzymes under direct electrochemical control. *Chem. Commun.* **2012**, *48*, 1400–1409. [[CrossRef](#)] [[PubMed](#)]
127. Ritter, M.; Anderka, O.; Ludwig, B.; Mantele, W.; Hellwig, P. Electrochemical and FTIR spectroscopic characterization of the cytochrome *bc₁* complex from *Paracoccus denitrificans*: Evidence for protonation reactions coupled to quinone binding. *Biochemistry* **2003**, *42*, 12391–12399. [[CrossRef](#)] [[PubMed](#)]
128. Baymann, F.; Robertson, D.E.; Dutton, P.L.; Mantele, W. Electrochemical and spectroscopic investigations of the cytochrome *bc₁* complex from *Rhodobacter capsulatus*. *Biochemistry* **1999**, *38*, 13188–13199. [[CrossRef](#)]
129. Kato, Y.; Sugiura, M.; Oda, A.; Watanabe, T. Spectroelectrochemical determination of the redox potential of pheophytin a, the primary electron acceptor in photosystem II. *Proc. Natl. Acad. Sci. USA* **2009**, *106*, 17365–17370. [[CrossRef](#)]
130. Nakamura, A.; Suzawa, T.; Kato, Y.; Watanabe, T. Species dependence of the redox potential of the primary electron donor P700 in photosystem I of oxygenic photosynthetic organisms revealed by spectroelectrochemistry. *Plant. Cell Physiol.* **2011**, *52*, 815–823. [[CrossRef](#)]
131. Haas, A.S.; Pilloud, D.L.; Reddy, K.S.; Babcock, G.T.; Moser, C.C.; Blasie, J.K.; Dutton, P.L. Cytochrome *c* and Cytochrome *c* Oxidase: Monolayer Assemblies and Catalysis. *J. Phys. Chem. B* **2001**, *105*, 11351–11362. [[CrossRef](#)]
132. Lee, C.-Y.; Reuillard, B.; Sokol, K.P.; Laftoglou, T.; Lockwood, C.W.J.; Rowe, S.F.; Hwang, E.T.; Fontecilla-Camps, J.C.; Jeuken, L.J.C.; Butt, J.N.; et al. A decahaem cytochrome as an electron conduit in protein-enzyme redox processes. *Chem. Commun.* **2016**, *52*, 7390–7393. [[CrossRef](#)]
133. Nowak, C.; Laredo, T.; Gebert, J.; Lipkowski, J.; Gennis, R.B.; Ferguson-Miller, S.; Knoll, W.; Naumann, R.L.C. 2D-SEIRA spectroscopy to highlight conformational changes of the cytochrome *c* oxidase induced by direct electron transfer. *Metallomics* **2011**, *3*, 619–627. [[CrossRef](#)]
134. Steinger, C.; Reiner-Rozman, C.; Schwaighofer, A.; Knoll, W.; Naumann, R.L.C. Kinetics of cytochrome *c* oxidase from *R. sphaeroides* initiated by direct electron transfer followed by tr-SEIRAS. *Bioelectrochemistry* **2016**, *112*, 1–8. [[CrossRef](#)]
135. Bogner, A.; Jouneau, P.-H.; Thollet, G.; Basset, D.; Gauthier, C. A history of scanning electron microscopy developments: Towards “wet-STEM” imaging. *Micron* **2007**, *38*, 390–401. [[CrossRef](#)] [[PubMed](#)]
136. Monsalve, K.; Roger, M.; Gutierrez-Sanchez, C.; Ilbert, M.; Nitsche, S.; Byrne-Kodjabachian, D.; Marchi, V.; Lojou, E. Hydrogen bioelectrooxidation on gold nanoparticle-based electrodes modified by *Aquifex aeolicus* hydrogenase: Application to hydrogen/oxygen enzymatic biofuel cells. *Bioelectrochemistry* **2015**, *106*, 47–55. [[CrossRef](#)] [[PubMed](#)]
137. Alsteens, D.; Gaub, H.E.; Newton, R.; Pfreundschuh, M.; Gerber, C.; Müller, D.J. Atomic force microscopy-based characterization and design of biointerfaces. *Nat. Rev. Mater.* **2017**, *2*, 17008. [[CrossRef](#)]
138. Connell, S.D.; Smith, D.A. The atomic force microscope as a tool for studying phase separation in lipid membranes. *Mol. Membr. Biol.* **2006**, *23*, 17–28. [[CrossRef](#)] [[PubMed](#)]
139. Goodchild, J.A.; Walsh, D.L.; Connell, S.D. Nanoscale Substrate Roughness Hinders Domain Formation in Supported Lipid Bilayers. *Langmuir* **2019**, *35*, 15352–15363. [[CrossRef](#)] [[PubMed](#)]
140. Aufderhorst-Roberts, A.; Chandra, U.; Connell, S.D. Three-Phase Coexistence in Lipid Membranes. *Biophys. J.* **2017**, *112*, 313–324. [[CrossRef](#)] [[PubMed](#)]
141. Frederix, P.L.T.M.; Bosshart, P.D.; Engel, A. Atomic force microscopy of biological membranes. *Biophys. J.* **2009**, *96*, 329–338. [[CrossRef](#)]
142. Carvalho, F.A.; Connell, S.; Miltenberger-Miltenyi, G.; Pereira, S.V.; Tavares, A.; Ariens, R.A.S.; Santos, N.C. Atomic force microscopy-based molecular recognition of a fibrinogen receptor on human erythrocytes. *ACS Nano* **2010**, *4*, 4609–4620. [[CrossRef](#)]

143. Heath, G.R.; Roth, J.; Connell, S.D.; Evans, S.D. Diffusion in low-dimensional lipid membranes. *Nano Lett.* **2014**, *14*, 5984–5988. [[CrossRef](#)]
144. Heath, G.R.; Scheuring, S. Advances in high-speed atomic force microscopy (HS-AFM) reveal dynamics of transmembrane channels and transporters. *Curr. Opin. Struct. Biol.* **2019**, *57*, 93–102. [[CrossRef](#)]
145. Hao, X.; Zhang, J.; Christensen, H.E.M.; Wang, H.; Ulstrup, J. Electrochemical single-molecule AFM of the redox metalloenzyme copper nitrite reductase in action. *ChemPhysChem* **2012**, *13*, 2919–2924. [[CrossRef](#)] [[PubMed](#)]
146. Tang, J.; Yan, X.; Huang, W.; Engelbrekt, C.; Duus, J.Ø.; Ulstrup, J.; Xiao, X.; Zhang, J. Bilirubin oxidase oriented on novel type three-dimensional biocathodes with reduced graphene aggregation for biocathode. *Biosens. Bioelectron.* **2020**, *167*, 112500. [[CrossRef](#)] [[PubMed](#)]
147. González Arzola, K.; Gimeno, Y.; Arévalo, M.C.; Falcón, M.A.; Hernández Creus, A. Electrochemical and AFM characterization on gold and carbon electrodes of a high redox potential laccase from *Fusarium proliferatum*. *Bioelectrochemistry* **2010**, *79*, 17–24. [[CrossRef](#)] [[PubMed](#)]
148. Ciaccafava, A.; Infossi, P.; Ilbert, M.; Guiral, M.; Lecomte, S.; Giudici-Ortoni, M.T.; Lojou, E. Electrochemistry, AFM, and PM-IRRAS spectroscopy of immobilized hydrogenase: Role of a hydrophobic helix in enzyme orientation for efficient H₂ oxidation. *Angew. Chem. Int. Ed.* **2012**, *51*, 953–956. [[CrossRef](#)]
149. Gutiérrez-Sanz, O.; Olea, D.; Pita, M.; Batista, A.P.; Alonso, A.; Pereira, M.M.; Vélez, M.; de Lacey, A.L. Reconstitution of respiratory complex I on a biomimetic membrane supported on gold electrodes. *Langmuir* **2014**, *30*, 9007–9015. [[CrossRef](#)]
150. Neupane, S.; de Smet, Y.; Renner, F.U.; Losada-Pérez, P. Quartz Crystal Microbalance with Dissipation Monitoring: A Versatile Tool to Monitor Phase Transitions in Biomimetic Membranes. *Front. Mater.* **2018**, *5*, 46. [[CrossRef](#)]
151. Giess, F.; Friedrich, M.G.; Heberle, J.; Naumann, R.L.; Knoll, W. The protein-tethered lipid bilayer: A novel mimic of the biological membrane. *Biophys. J.* **2004**, *87*, 3213–3220. [[CrossRef](#)]
152. Lam, K.B.; Irwin, E.F.; Healy, K.E.; Lin, L. Bioelectrocatalytic self-assembled thylakoids for micro-power and sensing applications. *Sens. Actuators B* **2006**, *117*, 480–487. [[CrossRef](#)]
153. Chen, H.; Dong, F.; Minteer, S.D. The progress and outlook of bioelectrocatalysis for the production of chemicals, fuels and materials. *Nat. Catal.* **2020**, *3*, 225–244. [[CrossRef](#)]
154. Ruff, A.; Conzuelo, F.; Schuhmann, W. Bioelectrocatalysis as the basis for the design of enzyme-based biofuel cells and semi-artificial biophotoelectrodes. *Nat. Catal.* **2020**, *3*, 214–224. [[CrossRef](#)]
155. Grattieri, M.; Beaver, K.; Gaffney, E.M.; Dong, F.; Minteer, S.D. Advancing the fundamental understanding and practical applications of photo-bioelectrocatalysis. *Chem. Commun.* **2020**, *56*, 8553–8568. [[CrossRef](#)] [[PubMed](#)]
156. Milton, R.D.; Minteer, S.D. Direct enzymatic bioelectrocatalysis: Differentiating between myth and reality. *J. R. Soc. Interface* **2017**, *14*, 20170253. [[CrossRef](#)] [[PubMed](#)]
157. Xiao, X.; Xia, H.-Q.; Wu, R.; Bai, L.; Yan, L.; Magner, E.; Cosnier, S.; Lojou, E.; Zhu, Z.; Liu, A. Tackling the Challenges of Enzymatic (Bio)Fuel Cells. *Chem. Rev.* **2019**, *119*, 9509–9558. [[CrossRef](#)] [[PubMed](#)]
158. Cooney, M.J.; Svoboda, V.; Lau, C.; Martin, G.; Minteer, S.D. Enzyme catalysed biofuel cells. *Energy Environ. Sci.* **2008**, *1*, 320–337. [[CrossRef](#)]
159. Minteer, S.D.; Liaw, B.Y.; Cooney, M.J. Enzyme-based biofuel cells. *Curr. Opin. Biotechnol.* **2007**, *18*, 228–234. [[CrossRef](#)]
160. Sheldon, R.A.; Woodley, J.M. Role of Biocatalysis in Sustainable Chemistry. *Chem. Rev.* **2018**, *118*, 801–838. [[CrossRef](#)]
161. Mazurenko, I.; Wang, X.; de Poulpiquet, A.; Lojou, E. H₂/O₂ enzymatic fuel cells: From proof-of-concept to powerful devices. *Sustain. Energy Fuels* **2017**, *1*, 1475–1501. [[CrossRef](#)]
162. Vincent, K.A.; Parkin, A.; Armstrong, F.A. Investigating and exploiting the electrocatalytic properties of hydrogenases. *Chem. Rev.* **2007**, *107*, 4366–4413. [[CrossRef](#)]
163. Plumeré, N.; Rüdiger, O.; Oughli, A.A.; Williams, R.; Vivekananthan, J.; Pöller, S.; Schuhmann, W.; Lubitz, W. A redox hydrogel protects hydrogenase from high-potential deactivation and oxygen damage. *Nat. Chem.* **2014**, *6*, 822–827. [[CrossRef](#)]
164. Ruff, A.; Szczeny, J.; Marković, N.; Conzuelo, F.; Zacarias, S.; Pereira, I.A.C.; Lubitz, W.; Schuhmann, W. A fully protected hydrogenase/polymer-based bioanode for high-performance hydrogen/glucose biofuel cells. *Nat. Commun.* **2018**, *9*, 3675. [[CrossRef](#)]

165. Vincent, K.A.; Cracknell, J.A.; Lenz, O.; Zebger, I.; Friedrich, B.; Armstrong, F.A. Electrocatalytic hydrogen oxidation by an enzyme at high carbon monoxide or oxygen levels. *Proc. Natl. Acad. Sci. USA* **2005**, *102*, 16951–16954. [[CrossRef](#)] [[PubMed](#)]
166. Vincent, K.A.; Cracknell, J.A.; Clark, J.R.; Ludwig, M.; Lenz, O.; Friedrich, B.; Armstrong, F.A. Electricity from low-level H₂ in still air—an ultimate test for an oxygen tolerant hydrogenase. *Chem. Commun.* **2006**, 5033–5035. [[CrossRef](#)] [[PubMed](#)]
167. So, K.; Kitazumi, Y.; Shirai, O.; Nishikawa, K.; Higuchi, Y.; Kano, K. Direct electron transfer-type dual gas diffusion H₂/O₂ biofuel cells. *J. Mater. Chem. A* **2016**, *4*, 8742–8749. [[CrossRef](#)]
168. Xia, H.-Q.; So, K.; Kitazumi, Y.; Shirai, O.; Nishikawa, K.; Higuchi, Y.; Kano, K. Dual gas-diffusion membrane- and mediatorless dihydrogen/air-breathing biofuel cell operating at room temperature. *J. Power Sources* **2016**, *335*, 105–112. [[CrossRef](#)]
169. Mano, N.; de Poulpique, A. O₂ Reduction in Enzymatic Biofuel Cells. *Chem. Rev.* **2018**, *118*, 2392–2468. [[CrossRef](#)]
170. Katz, E.; Willner, I.; Kotlyar, A.B. A non-compartmentalized glucose|O₂ biofuel cell by bioengineered electrode surfaces. *J. Electroanal. Chem.* **1999**, *479*, 64–68. [[CrossRef](#)]
171. Katz, E.; Willner, I. A biofuel cell with electrochemically switchable and tunable power output. *J. Am. Chem. Soc.* **2003**, *125*, 6803–6813. [[CrossRef](#)]
172. Wang, X.; Clément, R.; Roger, M.; Bauzan, M.; Mazurenko, I.; de Poulpique, A.; Ilbert, M.; Lojou, E. Bacterial Respiratory Chain Diversity Reveals a Cytochrome *c* Oxidase Reducing O₂ at Low Overpotentials. *J. Am. Chem. Soc.* **2019**, *141*, 11093–11102. [[CrossRef](#)]
173. Sakai, K.; Kitazumi, Y.; Shirai, O.; Takagi, K.; Kano, K. High-Power Formate/Dioxygen Biofuel Cell Based on Mediated Electron Transfer Type Bioelectrocatalysis. *ACS Catal.* **2017**, *7*, 5668–5673. [[CrossRef](#)]
174. Reda, T.; Plugge, C.M.; Abram, N.J.; Hirst, J. Reversible interconversion of carbon dioxide and formate by an electroactive enzyme. *Proc. Natl. Acad. Sci. USA* **2008**, *105*, 10654–10658. [[CrossRef](#)]
175. Milton, R.D.; Minteer, S.D. Enzymatic Bioelectrosynthetic Ammonia Production: Recent Electrochemistry of Nitrogenase, Nitrate Reductase, and Nitrite Reductase. *ChemPlusChem* **2017**, *82*, 513–521. [[CrossRef](#)] [[PubMed](#)]
176. Teodor, A.H.; Bruce, B.D. Putting Photosystem I to Work: Truly Green Energy. *Trends Biotechnol.* **2020**, *38*, 1329–1342. [[CrossRef](#)] [[PubMed](#)]
177. Friebe, V.M.; Frese, R.N. Photosynthetic reaction center-based biophotovoltaics. *Curr. Opin. Electrochem.* **2017**, *5*, 126–134. [[CrossRef](#)]
178. Koblizek, M.; Masojidek, J.; Komenda, J.; Kucera, T.; Pilloton, R.; Mattoo, A.K.; Giardi, M.T. A sensitive photosystem II-based biosensor for detection of a class of herbicides. *Biotechnol. Bioeng.* **1998**, *60*, 664–669. [[CrossRef](#)]
179. Swainsbury, D.J.K.; Friebe, V.M.; Frese, R.N.; Jones, M.R. Evaluation of a biohybrid photoelectrochemical cell employing the purple bacterial reaction centre as a biosensor for herbicides. *Biosens. Bioelectron.* **2014**, *58*, 172–178. [[CrossRef](#)]
180. Yehezkeili, O.; Tel-Vered, R.; Wasserman, J.; Trifonov, A.; Michaeli, D.; Nechushtai, R.; Willner, I. Integrated photosystem II-based photo-bioelectrochemical cells. *Nat. Commun.* **2012**, *3*, 781. [[CrossRef](#)]
181. Riedel, M.; Wersig, J.; Ruff, A.; Schuhmann, W.; Zouni, A.; Lisdat, F. A Z-Scheme-Inspired Photobioelectrochemical H₂O/O₂ Cell with a 1 V Open-Circuit Voltage Combining Photosystem II and PbS Quantum Dots. *Angew. Chem. Int. Ed.* **2019**, *58*, 801–805. [[CrossRef](#)]
182. Nam, D.H.; Zhang, J.Z.; Andrei, V.; Kornienko, N.; Heidary, N.; Wagner, A.; Nakanishi, K.; Sokol, K.P.; Slater, B.; Zebger, I.; et al. Solar Water Splitting with a Hydrogenase Integrated in Photoelectrochemical Tandem Cells. *Angew. Chem. Int. Ed.* **2018**, *57*, 10595–10599. [[CrossRef](#)]
183. Sokol, K.P.; Robinson, W.E.; Warnan, J.; Kornienko, N.; Nowaczyk, M.M.; Ruff, A.; Zhang, J.Z.; Reisner, E. Bias-free photoelectrochemical water splitting with photosystem II on a dye-sensitized photoanode wired to hydrogenase. *Nat. Energy* **2018**, *3*, 944–951. [[CrossRef](#)]
184. Sokol, K.P.; Robinson, W.E.; Oliveira, A.R.; Warnan, J.; Nowaczyk, M.M.; Ruff, A.; Pereira, I.A.C.; Reisner, E. Photoreduction of CO₂ with a Formate Dehydrogenase Driven by Photosystem II Using a Semi-artificial Z-Scheme Architecture. *J. Am. Chem. Soc.* **2018**, *140*, 16418–16422. [[CrossRef](#)]
185. Lubner, C.E.; Grimme, R.; Bryant, D.A.; Golbeck, J.H. Wiring photosystem I for direct solar hydrogen production. *Biochemistry* **2010**, *49*, 404–414. [[CrossRef](#)] [[PubMed](#)]

186. Tapia, C.; Milton, R.D.; Pankratova, G.; Minter, S.D.; Åkerlund, H.-E.; Leech, D.; De Lacey, A.L.; Pita, M.; Gorton, L. Wiring of Photosystem I and Hydrogenase on an Electrode for Photoelectrochemical H₂ Production by using Redox Polymers for Relatively Positive Onset Potential. *ChemElectroChem* **2017**, *4*, 90–95. [[CrossRef](#)]
187. Zhao, F.; Wang, P.; Ruff, A.; Hartmann, V.; Zacarias, S.; Pereira, I.A.C.; Nowaczyk, M.M.; Rögner, M.; Conzuelo, F.; Schuhmann, W. A photosystem I monolayer with anisotropic electron flow enables Z-scheme like photosynthetic water splitting. *Energy Environ. Sci.* **2019**, *12*, 3133–3143. [[CrossRef](#)]
188. Hancock, A.M.; Meredith, S.A.; Connell, S.D.; Jeuken, L.J.C.; Adams, P.G. Proteoliposomes as energy transferring nanomaterials: Enhancing the spectral range of light-harvesting proteins using lipid-linked chromophores. *Nanoscale* **2019**, *11*, 16284–16292. [[CrossRef](#)]
189. Liu, J.; Friebe, V.M.; Frese, R.N.; Jones, M.R. Polychromatic solar energy conversion in pigment-protein chimeras that unite the two kingdoms of (bacterio)chlorophyll-based photosynthesis. *Nat. Commun.* **2020**, *11*, 1542. [[CrossRef](#)]
190. Liu, J.; Mantell, J.; Jones, M.R. Minding the Gap between Plant and Bacterial Photosynthesis within a Self-Assembling Biohybrid Photosystem. *ACS Nano* **2020**, *14*, 4536–4549. [[CrossRef](#)]
191. Moehlenbrock, M.J.; Minter, S.D. Extended lifetime biofuel cells. *Chem. Soc. Rev.* **2008**, *37*, 1188–1196. [[CrossRef](#)]
192. Rideau, E.; Dimova, R.; Schwille, P.; Wurm, F.R.; Landfester, K. Liposomes and polymersomes: A comparative review towards cell mimicking. *Chem. Soc. Rev.* **2018**, *47*, 8572–8610. [[CrossRef](#)]
193. Discher, D.E.; Eisenberg, A. Polymer vesicles. *Science* **2002**, *297*, 967–973. [[CrossRef](#)]
194. Poschenrieder, S.T.; Schiebel, S.K.; Castiglione, K. Stability of polymersomes with focus on their use as nanoreactors. *Eng. Life Sci.* **2018**, *18*, 101–113. [[CrossRef](#)]
195. Beales, P.A.; Khan, S.; Muench, S.P.; Jeuken, L.J.C. Durable vesicles for reconstitution of membrane proteins in biotechnology. *Biochem. Soc. Trans.* **2017**, *45*, 15–26. [[CrossRef](#)] [[PubMed](#)]
196. Khan, S.; Li, M.; Muench, S.P.; Jeuken, L.J.C.; Beales, P.A. Durable proteo-hybrid vesicles for the extended functional lifetime of membrane proteins in bionanotechnology. *Chem. Commun.* **2016**, *52*, 11020–11023. [[CrossRef](#)] [[PubMed](#)]
197. Seneviratne, R.; Khan, S.; Moscrop, E.; Rappolt, M.; Muench, S.P.; Jeuken, L.J.C.; Beales, P.A. A reconstitution method for integral membrane proteins in hybrid lipid-polymer vesicles for enhanced functional durability. *Methods* **2018**, *147*, 142–149. [[CrossRef](#)]
198. Marušič, N.; Otrin, L.; Zhao, Z.; Lira, R.B.; Kyrilis, F.L.; Hamdi, F.; Kastiris, P.L.; Vidaković-Koch, T.; Ivanov, I.; Sundmacher, K.; et al. Constructing artificial respiratory chain in polymer compartments: Insights into the interplay between bo₃ oxidase and the membrane. *Proc. Natl. Acad. Sci. USA* **2020**, *117*, 15006–15017. [[CrossRef](#)] [[PubMed](#)]
199. Otrin, L.; Marušič, N.; Bednarz, C.; Vidaković-Koch, T.; Lieberwirth, I.; Landfester, K.; Sundmacher, K. Toward Artificial Mitochondrion: Mimicking Oxidative Phosphorylation in Polymer and Hybrid Membranes. *Nano Lett.* **2017**, *17*, 6816–6821. [[CrossRef](#)]
200. Smirnova, I.A.; Ädelroth, P.; Brzezinski, P. Extraction and liposome reconstitution of membrane proteins with their native lipids without the use of detergents. *Sci. Rep.* **2018**, *8*, 14950. [[CrossRef](#)]
201. Lee, S.C.; Knowles, T.J.; Postis, V.L.G.; Jamshad, M.; Parslow, R.A.; Lin, Y.-P.; Goldman, A.; Sridhar, P.; Overduin, M.; Muench, S.P.; et al. A method for detergent-free isolation of membrane proteins in their local lipid environment. *Nat. Protoc.* **2016**, *11*, 1149–1162. [[CrossRef](#)]
202. Kumar, A.; Hsu, L.H.-H.; Kavanagh, P.; Barrière, F.; Lens, P.N.L.; Lapinsonnière, L.; Lienhard V, J.H.; Schröder, U.; Jiang, X.; Leech, D. The ins and outs of microorganism–electrode electron transfer reactions. *Nat. Rev. Chem.* **2017**, *1*, 24. [[CrossRef](#)]
203. Rabaey, K.; Rozendal, R.A. Microbial electrosynthesis—Revisiting the electrical route for microbial production. *Nat. Rev. Microbiol.* **2010**, *8*, 706–716. [[CrossRef](#)]
204. Logan, B.E.; Rossi, R.; Ragab, A.; Saikaly, P.E. Electroactive microorganisms in bioelectrochemical systems. *Nat. Rev. Microbiol.* **2019**, *17*, 307–319. [[CrossRef](#)]
205. Jiang, Y.; Zeng, R.J. Bidirectional extracellular electron transfers of electrode-biofilm: Mechanism and application. *Bioresour. Technol.* **2019**, *271*, 439–448. [[CrossRef](#)] [[PubMed](#)]
206. Shi, M.; Jiang, Y.; Shi, L. Electromicrobiology and biotechnological applications of the exoelectrogens *Geobacter* and *Shewanella* spp. *Sci. China Technol. Sci.* **2019**, *62*, 1670–1678. [[CrossRef](#)]

207. Gregory, K.B.; Bond, D.R.; Lovley, D.R. Graphite electrodes as electron donors for anaerobic respiration. *Environ. Microbiol.* **2004**, *6*, 596–604. [[CrossRef](#)] [[PubMed](#)]
208. Geelhoed, J.S.; Stams, A.J.M. Electricity-assisted biological hydrogen production from acetate by *Geobacter sulfurreducens*. *Environ. Sci. Technol.* **2011**, *45*, 815–820. [[CrossRef](#)] [[PubMed](#)]
209. Ross, D.E.; Flynn, J.M.; Baron, D.B.; Gralnick, J.A.; Bond, D.R. Towards electrosynthesis in *shewanella*: Energetics of reversing the Mtr pathway for reductive metabolism. *PLoS ONE* **2011**, *6*, e16649. [[CrossRef](#)]
210. Le, Q.A.T.; Kim, H.G.; Kim, Y.H. Electrochemical synthesis of formic acid from CO₂ catalyzed by *Shewanella oneidensis* MR-1 whole-cell biocatalyst. *Enzyme Microb. Technol.* **2018**, *116*, 1–5. [[CrossRef](#)]
211. La Cava, E.; Guionet, A.; Saito, J.; Okamoto, A. Involvement of Proton Transfer for Carbon Dioxide Reduction Coupled with Extracellular Electron Uptake in *Shewanella oneidensis* MR-1. *Electroanalysis* **2020**, *32*, 1659–1663. [[CrossRef](#)]
212. Shin, H.J.; Jung, K.A.; Nam, C.W.; Park, J.M. A genetic approach for microbial electrosynthesis system as biocommodities production platform. *Bioresour. Technol.* **2017**, *245*, 1421–1429. [[CrossRef](#)]
213. Min, D.; Cheng, L.; Zhang, F.; Huang, X.-N.; Li, D.-B.; Liu, D.-F.; Lau, T.-C.; Mu, Y.; Yu, H.-Q. Enhancing Extracellular Electron Transfer of *Shewanella oneidensis* MR-1 through Coupling Improved Flavin Synthesis and Metal-Reducing Conduit for Pollutant Degradation. *Environ. Sci. Technol.* **2017**, *51*, 5082–5089. [[CrossRef](#)]
214. Yang, Y.; Ding, Y.; Hu, Y.; Cao, B.; Rice, S.A.; Kjelleberg, S.; Song, H. Enhancing Bidirectional Electron Transfer of *Shewanella oneidensis* by a Synthetic Flavin Pathway. *ACS Synth. Biol.* **2015**, *4*, 815–823. [[CrossRef](#)]
215. Glaven, S.M. Bioelectrochemical systems and synthetic biology: More power, more products. *Microb. Biotechnol.* **2019**, *12*, 819–823. [[CrossRef](#)] [[PubMed](#)]
216. Ueki, T.; Nevin, K.P.; Woodard, T.L.; Aklujkar, M.A.; Holmes, D.E.; Lovley, D.R. Construction of a *Geobacter* Strain With Exceptional Growth on Cathodes. *Front. Microbiol.* **2018**, *9*, 1512. [[CrossRef](#)] [[PubMed](#)]
217. La, J.A.; Jeon, J.-M.; Sang, B.-I.; Yang, Y.-H.; Cho, E.C. A Hierarchically Modified Graphite Cathode with Au Nanoislands, Cysteamine, and Au Nanocolloids for Increased Electricity-Assisted Production of Isobutanol by Engineered *Shewanella oneidensis* MR-1. *ACS Appl. Mater. Interfaces* **2017**, *9*, 43563–43574. [[CrossRef](#)] [[PubMed](#)]
218. Rowe, A.R.; Rajeev, P.; Jain, A.; Pirbadian, S.; Okamoto, A.; Gralnick, J.A.; El-Naggar, M.Y.; Nealon, K.H. Tracking Electron Uptake from a Cathode into *Shewanella* Cells: Implications for Energy Acquisition from Solid-Substrate Electron Donors. *mBio* **2018**, *9*, e02203-17. [[CrossRef](#)]
219. Tefft, N.M.; TerAvest, M.A. Reversing an Extracellular Electron Transfer Pathway for Electrode-Driven Acetoin Reduction. *ACS Synth. Biol.* **2019**, *8*, 1590–1600. [[CrossRef](#)]
220. Xie, Q.; Lu, Y.; Tang, L.; Zeng, G.; Yang, Z.; Fan, C.; Wang, J.; Atashgahi, S. The mechanism and application of bidirectional extracellular electron transport in the field of energy and environment. *Crit. Rev. Environ. Sci. Technol.* **2020**, *6*, 1–46.
221. Hasan, K.; Çevik, E.; Sperling, E.; Packer, M.A.; Leech, D.; Gorton, L. Photoelectrochemical Wiring of *Paulschulzia pseudovolvox* (Algae) to Osmium Polymer Modified Electrodes for Harnessing Solar Energy. *Adv. Energy Mater.* **2015**, *5*, 1501100. [[CrossRef](#)]
222. Bombelli, P.; Müller, T.; Herling, T.W.; Howe, C.J.; Knowles, T.P.J. A High Power-Density, Mediator-Free, Microfluidic Biophotovoltaic Device for Cyanobacterial Cells. *Adv. Energy Mater.* **2015**, *5*, 1–6. [[CrossRef](#)]
223. McCormick, A.J.; Bombelli, P.; Scott, A.M.; Philips, A.J.; Smith, A.G.; Fisher, A.C.; Howe, C.J. Photosynthetic biofilms in pure culture harness solar energy in a mediatorless bio-photovoltaic cell (BPV) system. *Energy Environ. Sci.* **2011**, *4*, 4699. [[CrossRef](#)]
224. Sekar, N.; Umasankar, Y.; Ramasamy, R.P. Photocurrent generation by immobilized cyanobacteria via direct electron transport in photo-bioelectrochemical cells. *Phys. Chem. Chem. Phys.* **2014**, *16*, 7862–7871. [[CrossRef](#)]
225. Zhang, J.Z.; Bombelli, P.; Sokol, K.P.; Fantuzzi, A.; Rutherford, A.W.; Howe, C.J.; Reisner, E. Photoelectrochemistry of Photosystem II in Vitro vs in Vivo. *J. Am. Chem. Soc.* **2018**, *140*, 6–9. [[CrossRef](#)] [[PubMed](#)]
226. Grattieri, M.; Patterson, S.; Copeland, J.; Klunder, K.; Minter, S.D. Purple Bacteria and 3D Redox Hydrogels for Bioinspired Photo-bioelectrocatalysis. *ChemSusChem* **2020**, *13*, 230–237. [[CrossRef](#)] [[PubMed](#)]
227. Pankratov, D.; Pankratova, G.; Gorton, L. Thylakoid membrane-based photobioelectrochemical systems: Achievements, limitations, and perspectives. *Curr. Opin. Electrochem.* **2020**, *19*, 49–54. [[CrossRef](#)]
228. Wenzel, T.; Härtter, D.; Bombelli, P.; Howe, C.J.; Steiner, U. Porous translucent electrodes enhance current generation from photosynthetic biofilms. *Nat. Commun.* **2018**, *9*, 1299. [[CrossRef](#)]

229. Sakimoto, K.K.; Wong, A.B.; Yang, P. Self-photosensitization of nonphotosynthetic bacteria for solar-to-chemical production. *Science* **2016**, *351*, 74–77. [[CrossRef](#)]
230. Cestellos-Blanco, S.; Zhang, H.; Kim, J.M.; Shen, Y.-X.; Yang, P. Photosynthetic semiconductor biohybrids for solar-driven biocatalysis. *Nat. Catal.* **2020**, *3*, 245–255. [[CrossRef](#)]
231. Hartshorne, R.S.; Reardon, C.L.; Ross, D.; Nuester, J.; Clarke, T.A.; Gates, A.J.; Mills, P.C.; Fredrickson, J.K.; Zachara, J.M.; Shi, L.; et al. Characterization of an electron conduit between bacteria and the extracellular environment. *Proc. Natl. Acad. Sci. USA* **2009**, *106*, 22169–22174. [[CrossRef](#)]
232. Shi, L.; Deng, S.; Marshall, M.J.; Wang, Z.; Kennedy, D.W.; Dohnalkova, A.C.; Mottaz, H.M.; Hill, E.A.; Gorby, Y.A.; Beliaev, A.S.; et al. Direct involvement of type II secretion system in extracellular translocation of *Shewanella oneidensis* outer membrane cytochromes MtrC and OmcA. *J. Bacteriol.* **2008**, *190*, 5512–5516. [[CrossRef](#)]
233. Ainsworth, E.V.; Lockwood, C.W.J.; White, G.F.; Hwang, E.T.; Sakai, T.; Gross, M.A.; Richardson, D.J.; Clarke, T.A.; Jeuken, L.J.C.; Reisner, E.; et al. Photoreduction of *Shewanella oneidensis* Extracellular Cytochromes by Organic Chromophores and Dye-Sensitized TiO₂. *Chembiochem* **2016**, *17*, 2324–2333. [[CrossRef](#)]
234. Hwang, E.T.; Sheikh, K.; Orchard, K.L.; Hojo, D.; Radu, V.; Lee, C.-Y.; Ainsworth, E.; Lockwood, C.; Gross, M.A.; Adschiri, T.; et al. A Decaheme Cytochrome as a Molecular Electron Conduit in Dye-Sensitized Photoanodes. *Adv. Funct. Mater.* **2015**, *25*, 2308–2315. [[CrossRef](#)]
235. Hwang, E.T.; Orchard, K.L.; Hojo, D.; Beton, J.; Lockwood, C.W.J.; Adschiri, T.; Butt, J.N.; Reisner, E.; Jeuken, L.J.C. Exploring Step-by-Step Assembly of Nanoparticle: Cytochrome Biohybrid Photoanodes. *ChemElectroChem* **2017**, *4*, 1959–1968. [[CrossRef](#)] [[PubMed](#)]
236. Rowe, S.F.; Le Gall, G.; Ainsworth, E.V.; Davies, J.A.; Lockwood, C.W.J.; Shi, L.; Elliston, A.; Roberts, I.N.; Waldron, K.W.; Richardson, D.J.; et al. Light-Driven H₂ Evolution and C=C or C=O Bond Hydrogenation by *Shewanella oneidensis*: A Versatile Strategy for Photocatalysis by Nonphotosynthetic Microorganisms. *ACS Catal.* **2017**, *7*, 7558–7566. [[CrossRef](#)]
237. Stikane, A.; Hwang, E.T.; Ainsworth, E.V.; Piper, S.E.H.; Critchley, K.; Butt, J.N.; Reisner, E.; Jeuken, L.J.C. Towards compartmentalized photocatalysis: Multiheme proteins as transmembrane molecular electron conduits. *Faraday Discuss.* **2019**, *215*, 26–38. [[CrossRef](#)] [[PubMed](#)]

Publisher's Note: MDPI stays neutral with regard to jurisdictional claims in published maps and institutional affiliations.



© 2020 by the authors. Licensee MDPI, Basel, Switzerland. This article is an open access article distributed under the terms and conditions of the Creative Commons Attribution (CC BY) license (<http://creativecommons.org/licenses/by/4.0/>).